Reviews in Mineralogy & Geochemistry
Vol. 89 pp. 373-400, 2023

Impact History of the Moon

Barbara A. Cohen[1], Carolyn H. van der Bogert[2], William F. Bottke[3], Natalie M. Curran[1,4], Caleb I. Fassett[5], Harald Hiesinger[2], Katherine H. Joy[6], Sara Mazrouei[7], Alexander Nemchin[8], Gregory A. Neumann[1], Marc D. Norman[9], Nicolle E. B. Zellner[10]

barbara.a.cohen@nasa.gov; vanderbogert@uni-muenster.de; bottke@boulder.swri.edu; natalie.m.curran@nasa.gov; caleb.i.fassett@nasa.gov; hiesinger@uni-muenster.de; katherine.joy@manchester.ac.uk; sara.mazrouei.seidani@mail.utoronto.ca; a.nemchin@curtin.edu.au; gregory.a.neumann@nasa.gov;marc.norman@anu.edu.au; nzellner@albion.edu

*[1]NASA Goddard Space Flight Center
Greenbelt, MD 20771, USA*

*[2]Institut für Planetologie
Westfälische Wilhelms–Universität
48149 Münster, Germany*

*[3]Southwest Research Institute
Boulder, CO 80302, USA*

*[4]Catholic University of America
NASA Goddard Space Flight Center
Greenbelt, MD 20771,USA*

*[5]NASA Marshall Space Flight Center
Huntsville, AL 35812, USA*

*[6]School of Earth and Environmental Sciences
University of Manchester
Manchester, M13 9PL, UK*

*[7]Department of Earth Sciences
University of Toronto
Toronto, Ontario M5S 3B1, Canada*

*[8]School of Earth and Planetary Sciences
Curtin University
Perth, Western Australia 6102, Australia*

*[9]Research School of Earth Sciences
The Australian National University
Canberra, ACT 0200, Australia*

*[10]Department of Physics
Albion College
Albion, MI 49224 USA*

1529-6466/23/0089-0009$05.00 (print)
1943-2666/23/0089-0009$05.00 (online)
http://dx.doi.org/10.2138/rmg.2023.89.09

1. INTRODUCTION

Establishing an absolute lunar impact chronology has important ramifications for understanding the early structure of the Solar System, to understand the evolution of both the dynamics and composition of the bodies. Our existing understanding of inner Solar System chronology is anchored to the crater density and analogy with impact flux rates on the Moon. The topic of lunar impact history has been the subject of numerous reviews (e.g., Hartmann et al. 2000; Ryder et al. 2000; Stöffler et al. 2006; Chapman et al. 2007; Fassett and Minton 2013; Bottke and Norman 2017; Zellner 2017; Hartmann 2019). In this chapter, we focus on examining new work in the last decade to constrain the lunar impact flux rates enabled by missions like the Lunar Reconnaissance Orbiter (LRO), the Gravity Recovery and Interior Laboratory (GRAIL), Chandrayaan-1, SELENE, and the Chang'E missions, as well as new results from Apollo, Luna, and meteorite samples made possible by increasingly sophisticated sample analysis techniques.

An important unresolved question is whether the lunar cratering rate declined monotonically since the Moon's formation, or whether there was a "terminal lunar cataclysm," (generalized to the Solar System as the "late heavy bombardment,") between about 3.8 and 4.1 Ga ago, where the rate and size of impacts increased to create the large lunar basins in a short period of time, well after Solar System formation. The possibility of a cataclysmic bombardment (Wetherill 1975) has been a central concept in planetary sciences since the 1960s, following detailed geological observations of the Moon and the discovery of petrological and geochemical evidence for intense shock metamorphism at ~3.9 Ga in many Apollo samples (Turner et al. 1973; Tera et al. 1974; Stöffler et al. 2006).

The last decade has given us an unprecedented look at the Moon from crust to core that gave us insight into the existence and structure of lunar basins, their degradation states, and stratigraphic relationships among them. Yet despite increasingly precise measurements of the isotopic ages of lunar samples and increasingly detailed geological studies of the lunar surface using high-resolution imaging, the absolute ages of almost all lunar basins are either unknown or poorly constrained. Evidence of earlier impacts may be masked in the available samples by the relatively late Imbrium basin-forming event (Hartmann 1975; Haskin et al. 1998; Chapman et al. 2007).

The heavily cratered terrains of the Moon and other bodies such as Mercury, Mars, and Callisto also provide clear physical evidence for an elevated flux of impactors across the Solar System that continued for several hundred million years after the initial accretion and differentiation of the terrestrial planets (Barr and Canup 2010; Fassett and Minton 2013). The dynamical models conceived to explain such a phenomenon encompass the gas–dust dynamics of forming disks and giant planet migration. These models are now invoked to understand not only our Solar System, but also systems of exoplanets around other stars. Such a phenomenon would also have affected the Earth at a point when other evidence shows that continents, oceans, and perhaps even life already existed. Though the high impact rate early in lunar history declined in the last 3 Ga, the importance of knowing the impact flux in the Earth–Moon system persists through the Cambrian, affecting evolving life on Earth, and to the present day, to evaluate the hazards impacts pose to astronauts and spacecraft.

2. THE BASIN-FORMING EPOCH: EVIDENCE FROM SAMPLES

Geologic observations of surface morphology and geophysical data have revealed at least 66 distinct basins and up to a few hundred candidate basins whose surface expressions have presumably been obscured by subsequent impact resurfacing (Wilhelms 1987; Spudis 1993; Frey 2011; Featherstone et al. 2013; Neumann et al. 2015). Cross-cutting relationships of ejecta and crater densities allow construction of a relative time-sequence of the basins that have a clear surface expression (Wilhelms 1987; Fassett et al. 2012). This basin stratigraphy is reasonably well established, although some significant uncertainties remain that will be discussed later (Table 1).

Despite increasingly precise measurements of the isotopic ages of lunar samples and increasingly detailed geological studies of the lunar surface using high-resolution imaging, the absolute ages of almost all lunar basins are either unknown or poorly constrained. In large part this reflects our inability to link individual lunar samples with specific basins or craters with a high degree of confidence. Stöffler et al. (2006) provided a comprehensive summary of the radiometric dates of lunar samples available at that time and their interpretation of the ages of key Nectarian and Imbrian basins. Updates to radiometric dates from samples and their association with basins is discussed in this section and summarized in Figure 1.

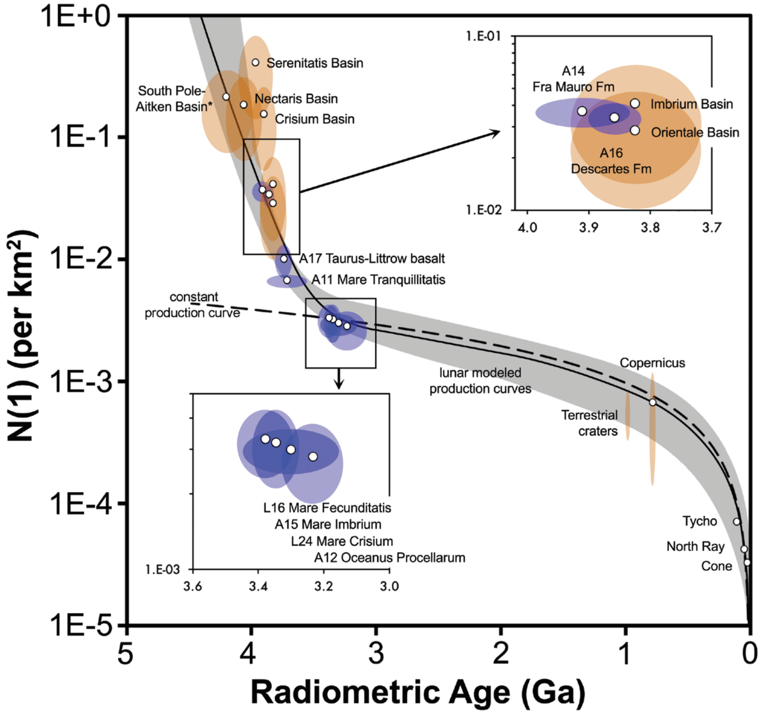

Figure 1. Lunar impact history from absolute ages of returned lunar rocks (billions of years old, or Ga) and the cumulative frequency of small (>1 km) craters per km^2 on the surfaces from which the samples were derived (after Hörz et al. 1991). The ellipse for each geologic unit encompasses the range of ages for returned samples and the uncertainty in crater density counts. Basins and craters are shown in orange while mare surfaces are shown in blue. The *N*(1) counts for lunar basins are derived from the *N*(20) counts in Fassett et al. (2012) using a scaling factor from Neukum and Ivanov (1994); all other *N*(1) values are from Hiesinger et al. (2023, this volume). Absolute ages for the basins reflect the ranges in Table 1, for all other formations, references are updated from sources in this chapter. The Neukum et al. (2001) lunar crater production curve is shown as a reference along with a (gray) envelope of all proposed production functions (discussed in detail in Hiesinger et al. 2023, this volume). Modeled crater production rates deviate from the curve representing a constant crater production rate around 4 Ga, implying a higher impact flux at that time, though the details of the curve are unconstrained at older ages.

2.1. Revisions to major basin ages during the "Late Heavy Bombardment" era

Central to this debate is the role of the Imbrium basin, which is the second largest and one of the youngest basins on the Moon. Until recently there has been a broad consensus among lunar geologists about the relationships of samples collected by the Apollo missions to the Imbrium, Serenitatis, and Nectaris basins. In that view, Apollo 14 sampled primary Imbrium ejecta,

Table 1. List of lunar basins in stratigraphic order and their radiometric ages

Basin Name	Age (Ga) 1974–1990	Age (Ga) 1991–2006	Age (Ga) 2009–present
South Pole-Aitken	~4.3–4.05	~4.3–4.05	4.4(?)–4.0
Serenitatis	4.45(?)–3.86	3.90	>4.1–3.83
Nectaris	~4.2–3.89	3.92–3.89	4.2 (?)–3.92
Crisium	~4.13–3.80	3.93–3.85	~3.9(?)
Imbrium	~3.99–3.85	3.85	3.93–3.72
Orientale	3.85–3.72	3.85–3.72	3.93–3.72

Note: Modified from Zellner 2017. Ages are from Nunes et al. (1974), Tera et al. (1974), Arvidson et al. (1976), Cadogan and Turner (1976), Drozd et al. (1977), Wilhelms (1987), Ryder (1990), Swindle et al. (1991), Bogard et al. (1994), Dalyrymple and Ryder (1993, 1996), Hartmann (2000), Ryder et al. (2000), Stöffler and Ryder (2001), Baldwin (2006), Koeberl (2006) and references therein, Hartmann (2019) and references therein, Norman (2009), Grange et al. (2010), Spudis et al. (2011), Fassett and Minton (2013), Mercer et al. (2015), and Bottke and Norman (2017) and references therein.

Apollo 17 sampled melt rocks formed by the Serenitatis event, and the Cayley and Descartes units at the Apollo 16 site were likely to be Imbrium and Nectaris ejecta, respectively (Stöffler et al. 2006). Today, the relationships between impact melt samples and their source basins for Apollo and Luna sites is still under active debate. The regional physiographic characteristics of the Fra Mauro formation (Apollo 14) were clearly sculpted by Imbrium, but it has been difficult to identify specific samples that unequivocally represent primary Imbrium ejecta (Spudis 1993; Stöffler et al. 2006; Merle et al. 2014). The best available age for Imbrium appears to be 3.92 ±0.01[1] Ga based on zircon and apatite from KREEP-rich breccias and melt rocks collected at the Apollo 12 and 14 sites (Nemchin et al. 2009; Liu et al. 2012; Snape et al. 2016; Merle et al. 2017).

Serenitatis basin ejecta was targeted for sampling by the Apollo 17 mission with the intent to date the formation of the Serenitatis basin, which is stratigraphically older than Imbrium and a key age in the context of understanding the magnitude and duration of the LHB. Attempts to date the fine-grained Apollo 17 melt rocks returned ^{40}Ar–^{39}Ar ages that were 20–40 million years older than the Apollo 14 and 15 breccias that were considered (at the time) as the best candidates for Imbrium ejecta (Dalrymple and Ryder 1993, 1996). This conclusion supported the idea that multiple basins formed within a narrow interval of time. However, the gas-release spectra were complex and the ages depend on weak plateaus (31–36% gas release) that in some cases were older than those of entrained clasts, which is geologically impossible (Jessberger et al. 1976; Dalrymple and Ryder 1996). An alternative interpretation is that the Apollo 17 melt rocks contain excess Ar possibly derived from assimilation of entrained clasts (Jessberger et al. 1976; Haskin et al. 1998), and, therefore, yield Ar ages marginally older than their primary formation. Recent studies have confirmed the complex distribution of Ar isotopes in Apollo 17 melt rocks (Mercer et al. 2015). Analysis of Lunar Reconnaissance Orbiter images of boulder tracks verified that the boulders that were sampled at Apollo 17 originated in outcrops within the North Massif walls, which had been interpreted as Serenitatis ejecta (Hurwitz and Kring 2016; Schmitt et al. 2017). However, these massifs and the Sculptured Hills deposits may be more closely related to Imbrium rather than Serenitatis (Spudis et al. 2011; Fassett et al. 2012), and U–Pb dating of Ca-phosphates in Apollo 17 melt breccias appears to support an Imbrium basin origin for these rocks (Thiessen et al. 2017; Zhang et al. 2019).

Even more challenging to interpret is the diverse suite of impact breccias and melt rocks collected at the Apollo 16 site. This mission targeted two regionally significant geological units with distinct physiography: the Cayley Plains and the Descartes Hills. The Cayley Plains appears to be related to the Fra Mauro formation (sampled at Apollo 14) and are generally accepted as Imbrium ejecta, possibly reworked by the addition of material from younger craters

[1]Ages are reported with significant figures and uncertainty levels in the original sources.

(Spudis 1993; Korotev 1994; Neukum et al. 2001; Stöffler et al. 2006; Joy et al. 2011). The origin of the Descartes unit is less certain; both Imbrium and Nectaris ejecta has been proposed (Head 1974; Muehlberger et al. 1980). The question is important because Nectaris is stratigraphically older than about a third of all of the lunar basins (Table 1), so the age of Nectaris would provide an important constraint on the timing and duration of the basin-forming epoch and the LHB.

Crystalline melt rocks and rock fragments were collected from the surface of the Cayley unit, but it is difficult to assign any of these samples to a specific geological unit (Vaniman et al. 1980; Norman et al. 2006; Fernandes et al. 2013). A set of relatively mafic (~17 wt.% Al_2O_3 bulk rock composition), poikilitic-textured melt rocks may be the best candidates for primary Imbrium ejecta (Korotev 1994; Norman et al. 2006). Crystallization ages of these melt rocks overlap within uncertainty the age inferred above for Imbrium (3.92–3.94 Ga; Stöffler et al. 1985; Norman et al. 2006; Norman et al. 2010), and their high concentrations of incompatible lithophile elements are consistent with a source in the Procellarum-KREEP Terrane. Other suites of Apollo 16 rocks contain impact-affected lithologies that are plausibly related to smaller, post-Imbrium craters ($D < 300$ km) in crustal terranes proximal to the Apollo 16 site (Niihara et al. 2019; Joy et al. 2020b).

More contentious is the geological significance of the Descartes unit, which has been interpreted as either Imbrium or Nectaris ejecta (Muehlberger et al. 1980; James 1981). The Descartes breccias differ from their Cayley counterparts in having lower-grade, fragmental or shock-metamorphosed matrices and highly aluminous (28–30 wt.% Al_2O_3) compositions with low concentrations of incompatible trace elements. Such compositions are similar to the feldspathic crust around Nectaris and contrast with the Procellarum-KREEP Terrane (Jolliff et al. 2000). James (1981) proposed an age of ~3.9 Ga for Nectaris, which would provide strong support for the terminal lunar cataclysm hypothesis. However, subsequent studies showed that the youngest population of clasts in the Descartes breccias is coeval with the KREEP-rich, crystalline melt rocks that are the best candidates for Imbrium ejecta, supporting geological observations that favor emplacement of the Descartes breccias as Imbrium ejecta. Interpreting the Descartes breccias as Imbrium ejecta removes the strongest argument for a young formation age of the Nectaris basin; without a young age for Nectaris, the constraint that all basins stratigraphically between Nectaris and Imbrium formed in a short window of time is significantly weakened, pulling the pin on the terminal lunar cataclysm (Table 1; Norman 2009; Norman et al. 2010).

The Descartes breccias are also intriguing because their low metamorphic grade has preserved evidence for earlier basin-scale impacts. Detailed petrologic, geochemical, and isotopic studies of a feldspathic lithology extracted from the Descartes breccia provide evidence for a basin-scale impact event at 4.22 $\pm$0.01 Ga, which may have been destroyed or obscured by Imbrium (Norman and Nemchin 2014; Norman et al. 2016). The ^{40}Ar–^{39}Ar ages of 4.1–4.2 Ga that are commonly observed in clasts and regolith pebbles around North Ray Crater (Maurer et al. 1978; Norman et al. 2010; Shuster et al. 2010; Fernandes et al. 2013) may reflect this putative pre-Imbrium basin rather than Nectaris (Norman et al. 2016).

Crisium is a multi-ring impact basin of Nectarian age, located in the northeastern portion of the lunar nearside (Head et al. 1978). Luna 24 succeeded in returning a 170-gram sample from Mare Crisium in 1976, which included a low-Ti basalt that is among the lowest Ti of any lunar basalt sampled. Luna 20 returned 55 g of samples from the highlands between Mare Fecunditatis and Mare Crisium. Among them were fragments interpreted to be Crisium impact melt, with radiometric ages ranging from ~3.84 Ga (Cadogan and Turner 1977; Stettler and Albarede 1978) to 3895 $\pm$17 Ma (Swindle et al. 1991). Additional ages for low-KREEP troctolites in the Luna 20 sample are 4191 $\pm$22 Ma and 4189 $\pm$8 Ma (Cohen et al. 2001). Updated Apollo 17 sample ages, also interpreted as representing Crisium impact-melt rocks, range from 3.88 to 3.93 Ga (Schmitt et al. 2017). While there is no agreement on which samples represent Crisium impact melt, the crater density on Crisium ejecta yields a model age of 3.99 Ga (Neukum 1984) and crater size–frequency distributions on the impact-melt deposits identified by Spudis and Sliz (2017) yields a younger age for the Crisium basin at 3.85–3.87 Ga (van der Bogert et al. 2017). It should be noted that there is significant uncertainty in ages modeled on production functions, depending on what constraints are assumed on terrains older than the mare surfaces (see Hiesinger et al. 2023, this volume). Wilhelms (1987) placed Crisium between Nectaris and Serenitatis, however, the uncertainty in the age of the Serenitatis basin does not help constrain the age of the Crisium basin.

In summary, current data provide compelling evidence that the basin-forming epoch extended back in time to at least 4.2 Ga and possibly earlier. The strong version of the terminal lunar cataclysm hypothesis in which all of the lunar basins formed within a brief interval (≤200 Ma; Ryder 2002) may be excluded as a viable hypothesis; however, samples do provide evidence for formation of multiple nearside basins in the period between 4.2 and 3.85 Ga even though the onset of the basin-forming epoch is still unconstrained. Imbrium ejecta appear to be more widespread on the lunar nearside than appreciated previously, and the perception of a terminal lunar cataclysm may have been biased by repeated (albeit unintentional) sampling of Imbrium ejecta at the various Apollo landing sites (Schaeffer and Schaeffer 1977; Haskin et al. 1998; Norman et al. 2010). Compositional variations within Imbrium ejecta may reflect complexities in radial ejecta distributions and the complex geology produced by such large events for which we have no terrestrial analogues. The lack of absolute ages, especially for the older lunar basins, and solid constraints on the mass vs. time flux of impactors across the inner Solar System, is a significant impediment to understanding the dynamical mechanisms that might have contributed to forming the lunar basins.

2.2. Evidence for earlier major impact events

Lunar samples interpreted to contain indirect evidence for ancient impact events is rarer than direct dating of impact-melt rocks. The interpretation of chronological data as representing impacts is based heavily on (i) the identification of textural and chemical characteristics of the analyzed rocks (or rock clasts found in the lunar breccia samples) that point towards an origin of these rocks/clasts as impact melts (Norman 2009) and (ii) the recognition of internal features found in some lunar zircon grains that formed as a result of impact related modification of zircon (e.g., Cavosie et al. 2015). In some cases, lunar zircon grains show two consistently different ages linked to different internal features (Pidgeon et al. 2007; Nemchin et al. 2009; Bellucci et al. 2016). Additionally, exploiting the low closure temperature of some chronometers such as ^{39}Ar–^{40}Ar in plutonic rocks has started to gain momentum (Shuster et al. 2010; Cassata et al. 2017). The main premise of this work is based on the assumption that the radiometric systems remain open for diffusion of daughter isotopes in the deep-seated plutonic rocks and require impact excavation to start the radiometric clock, thereby enabling dating of the major, possibly basin size, impact events.

In the terrestrial rocks, are several types of internal structures in the zircons that are directly linked to impacts (Timms et al. 2012). Some of these structures, such as planar deformation features (PDFs), twin and reidite lamellae, are too thin to be suitable for age determination, while others, for example deformation bands commonly show partial resetting of the U–Pb system (Cavosie et al. 2015). Only one type of impact related internal structure, granular zircon, has been shown to consistently determine impact ages in terrestrial rocks (e.g., Kenny et al. 2017). All of these internal features, with the exception of reidite, have been identified in lunar zircon grains as well (Crow et al. 2017).

In addition to the impact features known from the studies of terrestrial zircon, internal structures linked to impacts have been recognized in some lunar zircon grains, but which have not been found in terrestrial impact structures. For example, a complex zircon aggregate consisting of crystalline fragments surrounded by amorphous zircon "matrix" appears in an anorthosite clast from the breccia sample 73235. The "matrix zircon" was interpreted to represent a complete resetting of the U–Pb system during an impact and gave an age of 4187 ± 11 Ma, one hundred million years younger than the age of the fragments (Smith et al. 1986; Pidgeon et al. 2007; Bellucci et al. 2016). Another example is represented by a large (600 mm) zircon fragment from the breccia 72215 (Nemchin et al. 2009), which shows a recrystallization rim with an age of 4334 ± 10 Ma, significantly younger than the rest of the grain. Amorphous domains in the zircon from 73235 appear to form as a result of localized shock experienced by the grain during an impact, while the recrystallization rim in the grain from 72215 is likely to be a result of a prolonged heating in an impact ejecta blanket. Both features were identified as being impact-related in the lunar grains because of their marked age difference compared with other parts of the same grains and the assumed general lack of metamorphism and fluid induced alteration processes on the Moon. On Earth, similar internal structures may be created by metamorphic growth or radiation damage of U-rich parts of the grains.

The majority of lunar zircon grains, which are fragments found in breccia matrices, appear to be internally uniform and yield a single U–Pb age from multiple analyses. These ages are commonly interpreted as crystallization ages, but this interpretation remains ambiguous, as they may also represent the impact-reset ages from within larger, more complex grains broken apart during incorporation into their host breccias. Some of these fragments may also represent crystallization as a result of solidification of an impact melt, as in the case of zircon from sample 73217, which gave an age of 4335 ± 5 Ma (Grange et al. 2009). Though investigation of breccia grains does not provide definitive information regarding the size of these impacts, evidence of large (potentially basin-sized) impacts may be gained from zircon -related minerals in rocks derived from thick impact-melt sheets, for example, zirconolite yielded a Pb–Pb age of 4.22 ± 0.01 Ga in the coarse-grained lunar melt rock 67955, and microstructural evidence of high temperatures was recorded in 4.328 ± 8 Myr baddeleyite in troctolite 76535 (Norman and Nemchin 2014; White et al. 2020).

While the majority of ^{39}Ar–^{40}Ar ages represent the period of the late heavy bombardment (Section 2.1), there are numerous examples of older, impact-affected Ar–Ar sample ages obtained from Apollo 15, 16 and 17 sites and lunar meteorites (Shuster et al. 2010; Fernandes et al. 2013; Michael et al. 2018). However, of the rocks that have been investigated in combination with multiple chronometers, the ^{39}Ar–^{40}Ar ages are slightly younger than Sm–Nd, Rb–Sr, and U–Pb ages obtained on the same sample (Bouvier et al. 2015; Thiessen et al. 2017). While impact resetting may be a potential explanation for post-crystallization ^{39}Ar–^{40}Ar ages, other processes such as conductive cooling in the crust and magmatic overprints may play a role (Boehnke and Harrison 2016). ^{39}Ar–^{40}Ar thermochronometry offers means to assess whether ages obtained from exhumed crustal rocks can be ascribed to impact events, as well as potentially the size of the impact event responsible for resetting the Ar system. Detailed thermochronometry and modeling efforts have been used to examine multiple basin-sized impact events prior to 4.0 Ga, based on the basins' ability to exhume samples from deep within the lunar crust (Garrick-Bethell et al. 2009, 2020; Cassata et al. 2017).

Although the number of ages older than the proposed start time of the late heavy bombardment obtained by studies of lunar samples is limited, they appear to represent impact events around 4.2 and 4.3 Ga. Several lines of evidence support this, including the presence of large (>10 μm) neoblasts in some lunar zircon grains, which on Earth are commonly associated with mafic impact melts and the crater floor rocks in large (~250 km) impact structures, zircons and related minerals with old, impact-related ages, and ^{39}Ar–^{40}Ar ages of some plutonic rocks representing their extraction from significant depths in the lunar crust. Assigning these ages to specific impact structures is, however, tenuous on the basis of currently existing data.

2.3. Sample constraints from non-Apollo sources

Lunar meteorites provide another source of information about impact history from locations potentially far removed from Imbrium (Joy et al. 2023, this volume). Many lunar meteorites are regolith breccias that carry clasts of impact melt rocks. Although relatively few crystallization ages have been determined for these melt rock clasts, their distribution is broadly similar to that inferred from the Apollo samples and crater density studies of the lunar surface, with the oldest apparent ages around ~4.2 Ga, a peak at ~3.7 Ga, and a declining number of ages to ~2.5 Ga (Cohen et al. 2000, 2005; Joy and Arai 2013). As many of the feldspathic lunar meteorites are regolith breccias, the longer tail to younger ages in the meteorite clasts compared to the Apollo melt rocks may reflect smaller or more localized impact events than the basins sampled by the Apollo sites (Fig. 2).

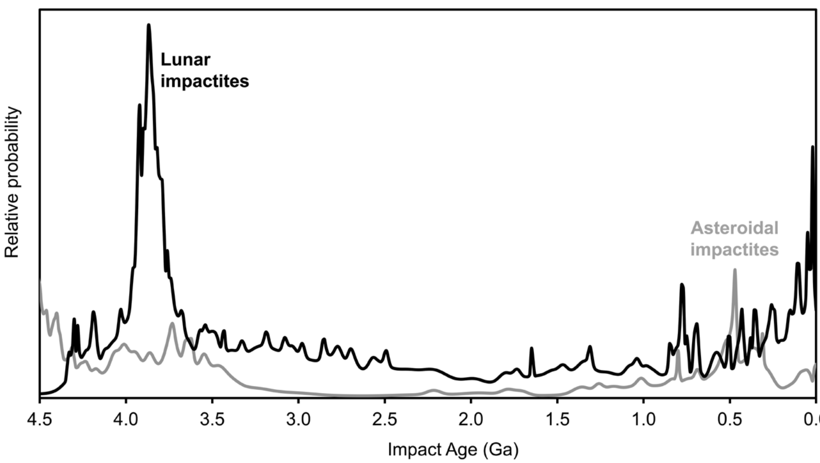

Figure 2. Radiometric ages for impact-affected lunar samples. Data from Zellner (2017), updated with sources in this chapter.

Additional constraints come from impact ages of meteorites derived from asteroid parent bodies (Fig. 2), largely based on $^{40}Ar–^{39}Ar$ data and U–Pb isotopic compositions of phosphates, as these systems are sensitive to relatively low-temperature events (reviewed in Bogard 2011; Jourdan 2012; Swindle et al. 2014). H-chondrites show a prominent group of reported $^{40}Ar–^{39}Ar$ ages between ~3.5 and 4.0 Ga, with the clast-poor, impact-melt rocks La Paz (LAP) 02240 and LAP 031125 yielding especially well-defined plateau ages of 3.939 ± 0.062 Ga and 3.942 ± 0.023 Ga, respectively (Swindle et al. 2009, 2014). Eucrites and howardites, believed to come from the asteroid 4 Vesta, have also yielded numerous impact-caused Ar ages between 3.4 and 4.1 Ga, with groups of ages at ~3.5 and 3.8–4.0 Ga, and few such ages between 4.1 and 4.5 Ga (Bogard 2011; Cohen 2013; Kennedy et al. 2013). The impact-melt clasts in howardites must have formed by high-velocity collisions (Cohen 2013; Marchi et al. 2013). Mesosiderites commonly yield Ar ages of 3.8 to 4.1 Ga, with a mean age of 3.94 ± 0.1 Ga for the 19 samples considered by Bogard (2011), although the very slow cooling experienced by these meteorites following disruption and re-accretion of their parent body complicates the interpretation of these data.

Few rocks older than 3.9 Ga exist on the Earth, so samples from the basin epoch are scarce. Detrital zircon grains identified in 3.3 Ga metasediments found in the Jack Hills of Western Australia, have a broad abundance peak between 3.9 and 4.2 Ga, with a maximum at 4.1 Ga (Blichert-Toft and Albarède 2008; Harrison 2009; Holden et al. 2009). Possible links between thermal events in these zircons and impacts between 4.1–3.9 Ga have been proposed (Trail et al. 2007; Abbott et al. 2012; Bell and Harrison 2013; Marchi et al. 2014), though there is some debate as to whether the zircons crystallized from wet, minimum-melt granites or impact-produced melt sheets (Harrison 2009; Kenny et al. 2017). Multiple impact-produced spherule beds have been found in terrestrial Archean and early Proterozoic terrains (Lowe et al. 2003; Simonson and Glass 2004). Models of Earth impactors and spherule formation yields size–frequency distributions for the expected spherule population similar to those observed, with an overall age distribution corresponding to the formation on the Earth of 70 to 80 craters with D > 150 km between 1.7 and 3.7 Ga (Bottke et al. 2012; Johnson and Melosh 2012). Given that the Earth has a gravitational cross section ~20× that of the Moon, these constraints would explain four such craters on the Moon formed in the period 3.0 to 3.7 Ga. Collectively, they suggest the LHB had a long-lived tail that potentially lasted down to ~2 Ga on Earth for Chicxulub-sized impact events, consistent with the distribution of impact ages in lunar meteorites (Cohen et al. 2000, 2005; Joy and Arai 2013).

2.4. Sources of lunar impactors

Establishing the sources of and changes in impactor populations responsible for basin and post-basin impact events provides critical constraints for understanding the causes of enhanced impact flux and for helping to develop models of the Solar System's dynamical evolution (see Section 4). Estimates of the proportion of material added to the Moon by impactors in the epoch of basin formation are in the range of 0.05 to 0.005% of the Moon's total mass, much smaller than the amount of material added to the Earth and Moon during the late veneer immediately following formation (Morgan et al. 2001; Morbidelli et al. 2012b; Marchi et al. 2014; Walker et al. 2015). Such impactors could include a wide variety of asteroid types, comets and planetary materials (including the possibility of Earth ejected debris; Armstrong et al. 2002; Crawford et al. 2008; Armstrong 2010) and the dust derived from any of these sources. The types of asteroids that are sampled at the present day on Earth as meteorites, or the proportion between cometary bodies and near Earth-cross asteroids, may not necessarily be similar to those that were responsible for the impact basins and craters on the Moon in the basin-forming epoch. Recent review papers on the topic of impactor sources are provided by Walker et al. (2015) and Joy et al. (2016).

Evidence for the parent-bodies of lunar basin-forming impactors comes from a combination of petrological, geochemical and isotopic studies of lunar samples (Morgan et al. 1972, 1974; Korotev 1987; James 1996; Kring and Cohen 2002; Norman et al. 2002; Puchtel et al. 2008; Fischer-Gödde and Becker 2012; Joy et al. 2012 ; Sharp et al. 2014; Liu et al. 2015; Walker et al. 2015; Gleißner and Becker 2017, 2019; McIntosh et al. 2020) coupled to remote sensing observations of lunar crater size density populations (Strom et al. 2005; Marchi et al. 2012).

Highly siderophile element (HSE) and isotopic analyses of impact melt breccias of known age provide indirect chemical fingerprinting of ancient impactors that have been mixed with lunar target rocks (Walker et al. 2015). There are potential complications involved in closed system fractionation of metallic phases in silicate melt systems (Gleißner and Becker 2017), but analysis of multiple aliquots of the same sample can be used to mitigate these effects and infer the impactor composition. The fingerprints of these impactors have a range of HSE compositions. Data from Apollo 14, 15, 16 and 17 impact melts (along with one lunar meteorite) imply that projectile compositions in the basin-forming epoch were often more fractionated relative to the HSE signatures that were added during the late veneer accretion (Walker et al. 2015; Day et al. 2016) and they are also not identical to the main types of ordinary chondrites meteorites that we have in the present-day meteorite population (Liu et al. 2015; Walker et al. 2015). The impactors range from those that were compositionally similar to primitive chondritic asteroids and those that were from differentiated planetary embryo cores (Kring and Cohen 2002; Fischer-Gödde and Becker 2012; Walker et al. 2015; Gleißner and Becker 2017). Notably non-chondritic signatures (superchonditic HSE/Ir and enrichment of Ru relative to Pt) are reported in Apollo 16 samples, consistent with high abundances of iron meteorite-like metal frequently observed in the Apollo 16 lunar regolith and impact breccias (Korotev 1987). This implies that a planetary embryo core material may be responsible for the Imbrium impact event collision, although as Walker et al. (2015) note, this final Imbrium impactor event added only a very limited HSE contribution to the generated impact melts. It is highly likely that mixing also occurred between these different components during melting of earlier ejecta deposits (Gleißner and Becker 2017); indeed, some metamorphic granulitic samples, that are thought to represent older impact materials, have chemical signatures that are more akin to some ordinary and carbonaceous chondrite meteorites types (Fischer-Gödde and Becker 2012; Walker et al. 2015). Although HSE contents and relative isotope abundances have not yet been determined for comets, the lunar impactor types inferred by these HSE methods are compositionally distinct from the types of primitive carbonaceous chondrites thought to be most akin to cometary materials (i.e., the CM or CI or Tagish Lake meteorite types; Brandon et al. 2005; Liu et al. 2015).

Fragments of exogenous contributions to the lunar regolith provide more direct evidence of the types of small bodies striking the Moon at different times (Armstrong et al. 2002; Chapman 2002; Rubin 2012; Joy et al. 2012, 2016, 2020a). The survivability of different types of projectiles on the Moon varies, controlled by such factors as impact velocity, where long and short period comets typically have higher collisional speeds (>20 km/s) compared with those of asteroids (~18 km/s on average). These velocities may have been different in the past than at the present day as the Moon was closer in orbit to the Earth's gravity well (Marchi et al. 2012). Other factors contributing to projectile survival include impact angle, where trajectories of <10º potentially account for higher survival rates (Pierazzo and Melosh 2000; Svetsov and Shuvalov 2015; Schultz and Crawford 2016); target material properties, as more porous target rocks may buffer impacts and enhance survival (Nagaoka et al. 2014; Svetsov and Shuvalov 2015; Avdellidou et al. 2016; Daly and Schultz 2016); and impactor physical properties, where volatile-rich projectiles like comets will lose much of their water and hydrated mineral components in the vapor plume (Artemieva et al. 2008; Ong et al. 2010; Svetsov and Shuvalov 2015).

To date only mm to sub-mm sized meteorite silicate and metal meteorite fragments have been found in lunar regolith samples (Joy et al. 2016) and, given the constraints of what we know of comets from silicate phases collected by the Stardust mission and stratospheric interplanetary dust particles (IDPs), no cometary silicate debris has been directly identified in lunar regolith samples. Our best view to the basin-forming epoch surface regolith record, where such an archive potentially resides, are through the "ancient" regolith breccias formed from soils >3.5 Ga (McKay et al. 1986; Joy et al. 2011). However, our geographic view is limited to samples from the Apollo 16 landing site (McKay et al. 1986; Joy et al. 2011, 2012; Fagan et al. 2014). The Apollo 16 ancient regolith breccias have so far only yielded only small ultramafic magnesian relics, which are chemically distinct from lunar materials, and may represent silicate debris from primitive chondritic meteorites (Joy et al. 2012).

The collective evidence from detection of primitive chondritic projectile relics in ancient Apollo 16 regolith breccias and HSE analyses of impact melt samples supports the likelihood that asteroid-type projectiles were delivered to the Moon in the latter stages of the basin-forming epoch and, therefore, favors models involving leftover planetesimals of the terrestrial planet region or asteroid collisions rather than comets or Kuiper belt objects (Kring and Cohen 2002; Norman et al. 2006; Walker et al. 2015). This observation is bolstered by observations that that that the current population of craters is consistent with asteroidal sources (Werner et al. 2002; Morota et al. 2008). However, there is a need to expand our knowledge base across the lunar surface; future lunar regolith research and exploration should make efforts to identify evidence for such impactors in order to chemically and isotopically identify their parent bodies.

3. THE BASIN-FORMING EPOCH: STRATIGRAPHIC RELATIONSHIPS

Establishing the sequence of lunar basins is important, since basin ejecta are critical markers in the stratigraphic framework for the Moon (Shoemaker et al. 1962). Basin relationships on the Moon's surface were established by geologic mapping between the early 1960s and mid-1980s and are summarized by (Wilhelms 1987). The ejecta and secondary craters from large, ~1000 km diameter basins like Imbrium or Orientale modified the surrounding crust at a hemispheric scale (Head et al. 2010). Smaller ~300–500-km impact basins have more regional effects, but form more frequently, so their stratigraphy is important as well. In conjunction with absolute ages derived from samples, constraining the stratigraphy of lunar basins can illuminate the impactor flux early in the inner Solar System. The methodology for using remote sensing data to untangle the sequence of basins relies on three main categories of observations: superposition and cross-cutting relationships, crater counting, and basin degradation state. The last decade of observations from LRO, GRAIL, and other missions has enabled progress on basin stratigraphy using each of these techniques.

The Lunar Orbiter Laser Altimeter (LOLA) in LRO and the GRAIL mission have created the basis for a global assessment of the crustal structure of the Moon and the history of impact structures with diameters exceeding ~200 km, including impact basins (Wieczorek et al. 2013; Zuber et al. 2013; Neumann et al. 2015; Smith et al. 2017). The impact process and subsequent gravitational rebound excavates and redistributes the lunar crust, leaving a characteristic signature of central thinning and peripheral thickening. Depending on the degree of isostatic relaxation and subsequent infilling, the resulting central free-air gravity signature may be strongly positive (mascons) or somewhat negative. However, a bandpassed Bouguer anomaly map (Fig. 3) shows a positive central anomaly indicating mantle uplift and thinned crust, usually encircled by an annular region of thickened crust resulting from processes within the transient cavity. As an example, the original cavity wall was not preserved in any of the topographic rings exposed at the surface of the Orientale multi-ring basin, but the size of such basins may be estimated from the diameter of the central Bouguer high, even in the most degraded cases where the main topographic rim can no longer be identified (Zuber et al. 2016). The size can be related by scaling laws to the original impact energy and thus the history and chronology of impact basins constrains dynamical models of the early Solar System, and to some extent, target thermal structure (Melosh 1989; Miljković et al. 2013; Baker et al. 2016).

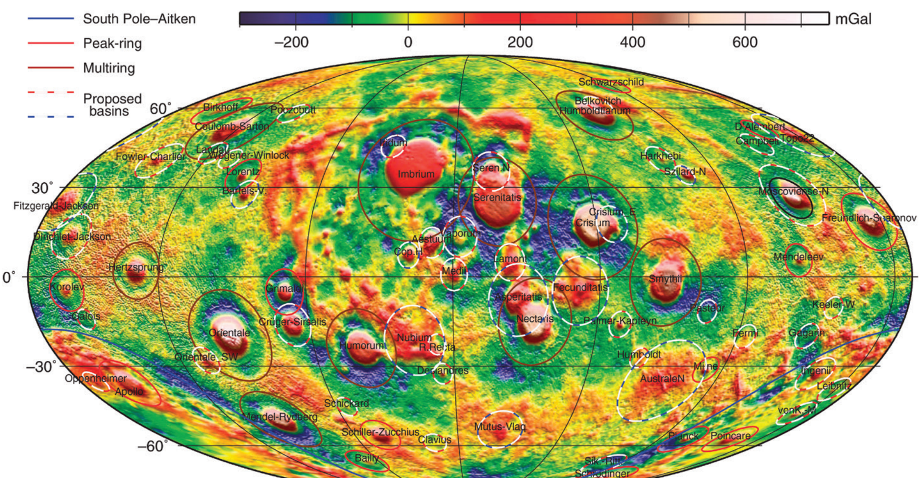

Figure 3. GRAIL Bouguer gravity anomaly map bandpassed from spherical harmonic degree 6-600 to emphasize basins, from Neumann et al. (2015) CC-BY-NC.

The GRAIL gravity data have provided substantial new clarity about what basins exist and the size of individual basins over the entire lunar surface. (Neumann et al. 2015) cataloged 43 basins with diameters greater than 300 km (Fig. 4), more than conservative estimates from LOLA data but fewer than some other pre-GRAIL estimates suggested (Frey 2011; Fassett et al. 2012; Featherstone et al. 2013). Previously-identified basins classified as "probable" or "uncertain" were relocated, downsized or eliminated while some new basins were added or confirmed on the basis of their clear gravity signature. In some cases, basin sizes were substantially revised. The population of basins with diameters less than 200 km is fitted well with the existing cumulative Hartmann–Neukum production function, but this function underestimates the basin population with diameters between 300 and 1000 km. Efforts to resolve impacts that have almost fully relaxed, have unusual gravity signatures, or have been buried under mare deposits, have turned up a few smaller proposed basins but do not generate overwhelming changes in the size–frequency distribution (Ishihara et al. 2011; Schultz and Crawford 2016; Sood et al. 2017). The cumulative distribution of basins $D > 300$ km has grown only slightly, not supporting models of impactors with a size distribution of the main asteroid belt (Strom et al. 2005); it is unlikely that the lunar surface could have been bombarded by enough main belt asteroids to produce the observed number of $D > 90$ km craters without producing many basins larger than Imbrium (Marchi et al. 2009; Minton et al. 2015).

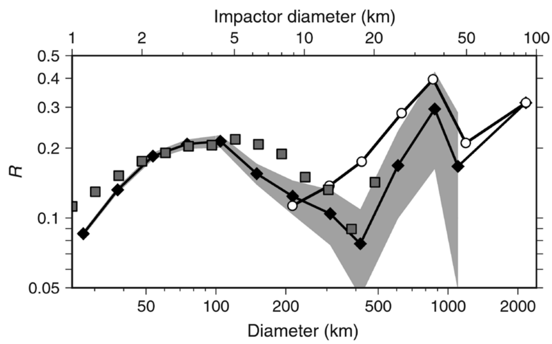

Figure 4. Strom's (2005) asteroid belt population size distribution (**squares**) aligned to match the R-plot density of GRAIL-determined basins (**circles**) at a diameter of 200 km, and the LOLA-derived (Head et al. 2010) catalog prior to GRAIL (**diamonds and gray field**). Adapted from Neumann et al. (2015) CC-BY-NC.

Crustal thickness maps of the Moon have revealed more large impact basins on the nearside hemisphere of the Moon than on its farside. One possible explanation for this asymmetry is differences in crustal properties (particularly temperature) at the time the basins formed (Miljković et al. 2013). However, the global asymmetry is still under debate, as the gravitational structure of the most ancient structures may be severely overprinted or completely absent. Some elongated gravity signatures or lineated features in topography have been proposed to represent fragments of oblique impact bodies rather than separate impact basins (Wichman and Schultz 1992; Schultz and Crawford 2016), while others hold that nearly-coincident impact structures may have been emplaced in different eras (Ishihara et al. 2011).

Measurements of the superposed crater population of basins are used to order the basin sequence (Hartmann and Wood 1971; Fassett et al. 2012; Fassett 2016). The main limiting factors in using this technique are that basins have a limited surface area, effects of later resurfacing can erase superposed craters (including deposition of maria), and uncertainties about the contribution of secondary craters (Hiesinger et al. 2023, this volume). Fassett et al. (2012) used LRO images and topography to re-examine both the relative stratigraphy and the crater statistics of ≥20 km craters superposed on 30 lunar basins larger than 300 km. Along with a substantially improved basemap for crater analysis, the Fassett et al. (2012) study used a buffered crater counting approach to partially counteract the effects of later resurfacing of basins by maria. The major conclusion from that study was that the "standard" sequence of lunar basins developed by Wilhelms (1987) was qualitatively supported, although there were many more superposed craters on these basins than was originally recognized.

A major question reinvigorated by recent mission data has been the relative stratigraphic position of the Serenitatis basin. The highlands materials sampled at the Apollo 17 landing site were located at the most prominent Serenitatis ring, so its samples were used to argue that Serenitatis must be relatively young (i.e., Nectarian in age, slightly older than Imbrium; see Section 2.1). Spudis et al. (2011) used LROC data to re-examine the morphology of the Sculptured Hills from which the Apollo 17 samples are collected, making the argument that the Sculptured Hills are likely Imbrium ejecta rather than Serenitatis ejecta. Moreover, they point out that the numerous large craters on the eastern Serenitatis rim would be more consistent with an older pre-Nectarian age, an argument also supported by Fassett et al. (2012). If correct, this would mean that the presumed connection between the Apollo 17 samples and Serenitatis is incorrect. On the other hand, Evans et al. (2016) used GRAIL data to search for craters that formed after Serenitatis (and other basins) that were then buried by mare, and found that Serenitatis had relatively few buried superposed craters ≥90 km. This supports the original interpretation that Serenitatis is Nectarian in age. This particular region of the Moon is challenging for basin stratigraphy based on either cross-cutting relationships or visible crater statistics, because Imbrium basin's ejecta influenced the surrounding region so profoundly.

The relative degradation state between basins is also an indicator of their relative age. This arises because the topography, morphology, and interior structure of younger basins are less modified by later processes compared to those of older basins. Developing the sequence of basins based on their apparent morphological degradation state has been attempted using Lunar Orbiter observations (Stuart-Alexander and Howard 1970) and has also been extended to analyzing the gravity signature of basins to show that the crustal thickness contrast between the interior of a basin and its surroundings decreases with age (Neumann et al. 1996; Kamata et al. 2015; Conrad et al. 2016). The implication of these studies is that during the pre-Nectarian epoch, basin relaxation was an important process. Additionally, the nearside hemisphere is dominated by the Procellarum region, a 3,200-km diameter quasi-circular tectonomagmatic feature (Andrews-Hanna et al. 2014). The unique thermal history of the Procellarum region likely modified or erased ancient nearside basins, also potentially accounting for the paucity of lunar impact-melt rocks older than 4.2 Ga in the nearside lunar sample collections (see Section 2.1).

4. DYNAMICAL MODELS FOR THE BASIN-FORMING EVENTS

There are two major classes of dynamical scenarios that are frequently invoked to describe early bombardment of the Moon. Both assume that lunar bombardment is not merely a local affair but instead is strongly linked to the processes describing the endgame of planet formation. A successful model must not only explain what is found on the Moon but also early bombardment constraints identified on Mercury, Earth, Mars, the asteroids, and potentially bodies in the outer Solar System as well. The history of dynamical models applied to lunar bombardment is more fully presented in Bottke and Norman (2017).

The first scenario is a "declining bombardment" produced by a population of planetesimals left over from accretion that was dynamically excited by protoplanets and planetary embryos (Wetherill 1975; Turner 1979; Morbidelli et al. 2001, 2018; Chambers and Lissauer 2002; Bottke et al. 2007; Ćuk et al. 2010; Ćuk 2012). This population may include outer Solar System bodies injected into the inner Solar System by early giant planet migration within a gas disk (Walsh et al. 2011; Raymond and Izidoro 2017) or the early dynamical depletion of the primordial asteroid belt by planet formation processes (Morbidelli et al. 2015; Nesvorný et al. 2017). A declining bombardment would produce a monotonically decreasing impactor population over a timescale set by the planet formation model invoked. In many scenarios, it is assumed it could produce large lunar impacts for hundreds of Myr or more.

The second scenario is an "instability-driven bombardment" caused by late giant planet migration well after the solar nebula had dissipated. This violent rearrangement would be capable of destabilizing Kuiper belt and asteroid reservoirs across the Solar System (Fernandez and Ip 1984; Thommes et al. 1999; Levison et al. 2001). A quantified and well-developed description of this behavior is provided by the "Nice model" (Fig. 5; Gomes et al. 2005; Morbidelli et al. 2005; Tsiganis et al. 2005; Lega et al. 2013). In the Nice model, the giant planets are assumed to have formed in a more compact configuration between 5 and ~17 AU. They were surrounded by a primordial disk of small icy planetesimals, the ancestor of today's Kuiper belt, residing between ~20 and 30 AU. The net mass of the disk was several tens of Earth masses. Slow migration of the planets was induced by gravitational interactions with these icy planetesimals or collisionally-produced dust leaking out of the disk. Eventually, this triggered an instability that led to a violent reorganization of the outer planets. Uranus and Neptune were scattered into the primordial disk, flinging its members throughout the Solar System. The instability also drove resonances across the asteroid belt, driving substantial portions of it onto planet-crossing orbits. The majority of impacts on outer Solar System worlds would have been from comets, while those on the terrestrial planets and Moon would have been from both asteroids and those comets that survived passage into the inner Solar System.

The timing of the Nice model type of instability is unknown; it could potentially occur after a delay of several tens of Myr (early instability) or as long as many hundreds of Myr (late instability). In an early instability, the Nice model becomes yet another component of the aforementioned declining bombardment. In a late instability, the Nice model would produce a surge in lunar impacts hundreds of Myr after the formation of the Moon. This would come in two phases: Kuiper-belt objects would strike over a few tens of Myr immediately after the instability, while asteroids would continue to trickle out of the main belt over many hundreds of Myr. At present, dynamical models favor early instabilities over late ones, though considerable work needs to be done on modeling the trigger event (Nesvorný and Vokrouhlický 2016). It is also possible that a late Nice model would modify the orbits of the terrestrial planets, though this could be a necessary step in reproducing their observed orbits (Agnor and Lin 2012; Roig and Nesvorný 2015; Kaib and Chambers 2016).

At present, there is an ongoing debate about whether the early Moon experienced a declining bombardment, an instability-driven bombardment, or some combination of the two (for example, a "sawtooth" structure; Turner 1979; Morbidelli et al. 2012a). A hybrid model, where there are both early and late components of bombardment, currently appears to do the best job of matching constraints (Marchi et al. 2013; Bottke and Norman 2017; Morbidelli et al. 2018). The early component would be a relatively short-lived declining bombardment initiated during the planet formation era, with most impactors eliminated by collisional and dynamical evolution by ~4.4 Ga. Most Pre-Nectarian and potentially some older Nectarian-era lunar basins would be created at this time. The later component would come from a Nice model-like late instability that would start ~4.0 Ga to perhaps 4.2 Ga. It would be responsible for the many Nectarian-era and Imbrian-era basins and craters and the majority of Late Imbrian and early Eratosthenian-era craters.

5. POST-BASIN EPOCH TO PRESENT

The impact flux (Fig. 1) in the epoch between the formation of Imbrium (~3.9 Ga) and ~3 Ga must have been substantially higher than after 3 Ga (Neukum et al. 2001). This constraint arises from differences in crater density on the mare: the factor of ~1.7 times as many craters on the ~3.8 Ga unit at Apollo 11 compared to the ~3.2 Ga surface at Luna 24 (Robbins 2014; Wang et al. 2015). This is also supported by sample measurements on other lunar surfaces and by constraints on the age of the youngest large craters and basins. There is no strong observational evidence that demands a major alteration in the crater flux over long-time scales since the beginning of the Eratosthenian; though some amount of clustering in time is physically plausible as asteroidal breakup events could trigger epochs with higher rates, evidence of these events may average out over millions to billions of years (McEwen et al. 1997; Morota et al. 2009; Basilevsky and Head 2012; Fassett and Thomson 2014).

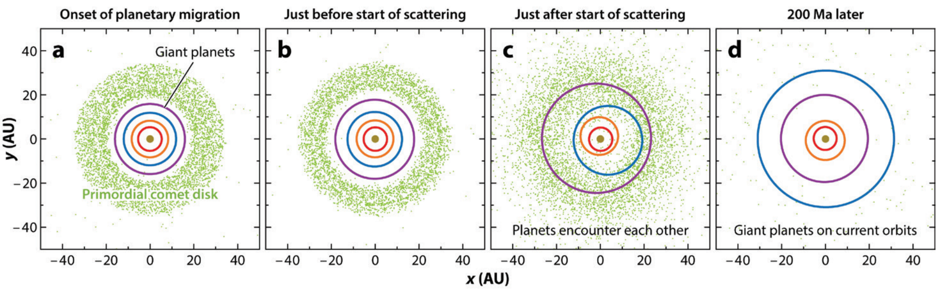

Figure 5. Planetary orbits and disk particle positions in the Nice model (from Bottke and Norman 2017). The panels show four different times from a reference simulation. In this run, the giant planets were initially on nearly-circular, co-planar orbits with semi-major axes of 5.5, 8.2, 11.5, and 14.2 AU. The initial disk contained 35 Earth masses between 15.5 and 34 AU. **(a)** Beginning of planetary migration, **(b)** Just prior to the dynamical instability of the giant planets, **(c)** During the instability, and **(d)** 200 Myr later, with the final planet orbits. The timing of the instability is unknown. This event also triggers the loss of asteroids from the primordial asteroid belt.

5.1. Constraints from crater counting and rock breakdown

Lunar chronology is constrained over the last 3 Ga by lunar mare basalt flows and younger benchmark craters where samples yield radiometric sample ages, including Copernicus, Tycho, North Ray, and Cone craters (Stöffler and Ryder 2001). The higher resolution imaging of the Moon made available by LROC, SELENE, and Chang'E-1 has been used to update the crater size–frequency distribution (CSFD) ages of these key lunar terrains (Hiesinger et al. 2003, 2012, 2016; Haruyama et al. 2009; Robbins 2014; Williams et al. 2014; Morota et al. 2015; Wang et al. 2015). A more detailed discussion of advances in crater-counting techniques and results for different lunar units can be found in Hiesinger et al. (2023, this volume).

A constant flux model for recent lunar periods can be used to fit the radiometric and exposure ages of Cone, North Ray, Tycho, and Copernicus craters along with the mare surfaces at Apollo 12, Apollo 15, Luna 16, and Luna 24 (Hiesinger et al. 2012; Williams et al. 2014). However, the (Robbins 2014) results differ by a factor of 2–3 for the area surrounding North Ray crater, and factoring in other landing sites, Robbins (2014) presented a revised chronology where a lunar surface previously modeled at 3 Ga may have an updated model crater age as young as 1.9 Ga.

Crater size–frequency distribution measurements of Copernicus crater and one of its rays show that Copernicus has significantly lower cumulative crater frequencies than previously thought, yielding a model age of 797 Ma, which fits existing lunar absolute chronologies significantly better than the results of previous counts (Hiesinger et al. 2012). Tycho crater is dated at ~124 Ma old, North Ray crater at ~46 Ma old, and Cone crater is ~39 Ma old (Hiesinger et al. 2012, 2016). Recent U–Pb ages of zircon and phosphate grains of 1.4 and 1.9 Ga from sample 15405 have been interpreted by (Grange et al. 2013) as the formation ages of Aristillus and Autolycus, respectively, which are slightly (200 Myr) younger than radiometric ages previously proposed for these craters on the basis of ^{40}Ar–^{39}Ar ages of shocked Apollo 15 KREEP basalt samples (Bernatowicz et al. 1978; Ryder et al. 1991). However, new crater size–frequency distributions for individual parts of the Autolycus ejecta blanket and crater floor yielded a wide range of model ages, none of which corresponded to either set of Apollo 15 sample ages (Hiesinger et al. 2016). This implies either that the dated samples are not related to Autolycus or that the crater measurements are so heavily affected by resurfacing and secondary cratering from Aristillus that they do not represent the formation age of Autolycus.

Lunar crater chronology may be refined by incorporating the relative crater degradation state. (Soderblom 1970; Soderblom and Lebofsky 1972) derived a degradation model from a simple diffusion equation. In the Apollo era, the data were so limited that this model was not fully applied for classifying the crater degradation status of mare units. But more recently, high resolution image and DTM data enabled application of the model to widespread mare units (Fassett and Thomson 2014).

An alternative method to crater counting for estimating the age of Copernican craters is rock abundance derived from the LRO Diviner thermal radiometer data (Bandfield et al. 2011). This method relies on the differing thermophysical characteristics of impact ejecta, where blocks larger than ~1 m remain warm through the lunar night whereas the regolith cools quickly. (Ghent et al. 2014) determined an inverse relationship between the rock abundance in large craters' ejecta and their age, as blocky ejecta is demolished by micrometeorite impacts and thermal cracking and becomes indistinguishable from regolith for craters older than ~1 Gyr. This suggests that the population of rocky craters is a reasonable quantitative definition for Copernican-era craters. Using this method, Mazrouei et al. (2017) determined the ages of young rocky craters suggested that the lunar cratering rate has increased by a factor of ~2–3 in the last ~250 Myr relative to the preceding ~750 Myr.

5.2. Lunar impact glass samples

Lunar impact glass samples, spherules and fragments formed in impact ejecta during ballistic flight, can provide important constraints on the Moon's impact history. These samples have the general composition of the target material (Delano 1991; Symes et al. 1998; Zellner et al. 2002) but degas during the impact-melting event, enabling dating of impact events by noble-gas methods (Culler et al. 2000; Muller et al. 2001; Delano et al. 2007; Zellner et al. 2009b). The size of the crater that creates these glasses is currently debated; suggestions for the size of the source crater range from 1 km to >100 km in diameter (Delano 1991; Hörz and Cintala 1997; Levine et al. 2005; Zeigler et al. 2006; Korotev et al. 2010; Norman et al. 2012).

Lunar impact glass can be distinguished from volcanic material by careful analysis of the major elements TiO_2 and Cr_2O_3 (Delano 1986). In general, impact glasses that possess higher abundances of FeO and TiO_2 are more likely to survive ballistic flight and eons of bombardment and regolith gardening, as well as be more resistant to the effects of diurnal heating of the lunar surface that can affect how well argon isotopes are retained in the glass (Gombosi et al. 2015). As a result, the glass shape, size, and composition are important characteristics to consider when using lunar impact glasses as tools for understanding the lunar bombardment rate (Zellner and Delano 2015).

Multiple populations of impact glass with ages >3500 Ma have been identified (Culler et al. 2000; Muller et al. 2001; Levine et al. 2005; Zellner and Delano 2015), similar to the trend exhibited by lunar meteorite clasts and terrestrial spherule beds (see Section 2.3). However, impact glass with ^{40}Ar–^{39}Ar ages ~800 Ma have also been identified in several Apollo regolith samples (Levine et al. 2005; Zellner et al. 2009b). While this age is coincident in time with the formation of Copernicus crater (Bogard et al. 1994; Barra et al. 2006), the impact glass samples have compositions different from the bulk regolith surrounding Copernicus, suggesting that multiple craters may have formed at this time.

5.3. Regolith breccias and solar wind implantation

Regolith breccias formed <3.5 Ga provide a window to understanding the sources of Earth–Moon-crossing impactor populations during a window of declining bombardment rates (Joy et al. 2011, 2012; Fagan et al. 2014). These younger samples potentially provide an archive of the types of Near Earth Objects that played a role in episodic mass extinction events here on Earth (Wetherill 1975). They also allow cross-correlation with discoveries of terrestrial fossil meteorites such as those found in Ordovician sediments (Heck et al. 2008, 2010), believed to have been derived from the breakup of an asteroid like the L-chondrite parent body (Haack et al. 1996).

As every particle within a sampled regolith could have seen distinct recycling histories, determining bulk regolith ages to constrain when projectiles were delivered is challenging. For surface regolith, one estimate of the maximum length of time that surface was exposed to space could be taken as the formation age of the underlying geological unit; however, localized lateral and vertical mixing often render this assumption too simplistic. The total length of time that a regolith sample has been exposed directly to space can be estimated using indicators such as implanted solar wind ^{36}Ar (Cohen et al. 2001; Eugster et al. 2001), the qualitative I_s/FeO maturity indicator (Morris 1978; Lucey et al. 2000); the residence time of samples in the upper regolith can be calculated using stable cosmogenic isotopes (e.g., ^{3}He, ^{21}Ne, ^{38}Ar, ^{81}Kr, ^{126}Xe) and knowledge of the composition (Eberhardt et al. 1976; Eugster et al. 2001; Lorenzetti et al. 2005; Curran et al. 2020). However, these methods do not tell us when the exposure event(s) occurred. Some authors have proposed that the ratio of parentless (non-radiogenic) ^{40}Ar, degassed from the lunar interior, to the ^{36}Ar in bulk soils and regolith breccias implanted by the solar wind, can be used as a semi-quantitative measure of the last time the soil was exposed to the solar wind (Eugster et al. 1973, 1983; McKay et al. 1986; Joy et al. 2011; Fagan et al. 2014). Others have suggested alternative mechanisms for implantation of orphan ^{40}Ar (Ozima et al. 2004; Korochantseva et al. 2016) and the accuracy of the temporal quantification index (Wieler 2016). Moreover, as in the case of present day soils, upper age estimates on regolith antiquity ages are challenging to constrain (Joy et al. 2016).

5.4. Current meteoroid impact rate

The present-day flux of large meteoroids on the lunar surface has been derived from both models and observational techniques, including seismic data of impacts and impact flash detections (a comprehensive review can be found in Oberst et al. 2012). Amateur and professional observatories currently monitor the Moon for light flashes, interpreted to represent impact events (Ortiz et al. 2000, 2006; Yanagisawa and Kisaichi 2002; Madiedo et al. 2014). ESA and NASA lunar impact monitoring programs have recorded over 400 flashes assumed to be meteoroid impacts since 2006 (Suggs et al. 2014; Xilouris et al. 2018; Avdellidou and Vaubaillon 2019). One of the brightest recorded flashes was later associated with a new 18.8 m crater observed by the Lunar Reconnaissance Orbiter Camera (LROC) Narrow Angle Camera (NAC) (Robinson et al. 2015). LROC NAC temporal image pairs have also been used to quantify the contemporary rate of crater production on the Moon, revealing 222 new impact craters in the period 2009–2015, higher than predicted by standard production functions for the Moon (Speyerer et al. 2016). During several of the known meteoroid showers, the Lunar Dust Experiment (LDEX) on the Lunar Atmosphere and Dust Environment Explorer (LADEE) observed temporary enhancements of the lunar dust cloud, localized to the hemisphere exposed to the incident meteoroid shower flux; approximately 40 μm per million years of lunar soil is estimated to be redistributed from meteoritic bombardment (Szalay and Horányi 2016).

6. SUMMARY AND FUTURE WORK

The lunar bombardment record is a crucial component in understanding Solar System history, the architecture of the planets, and the redistribution of energy into planetary surfaces. However, it also encompasses an enduring controversy, as evidenced by multiple recent papers. Revisions to the geologic setting of the Apollo sample-collection sites and continued sample characterization have weakened the case for a single sharp spike in impact flux, or terminal lunar cataclysm. Instead, many of the 3.9 Ga ages in lunar samples, particularly in the Apollo collection, likely represent the age of the Imbrium basin. However, there exist many published impact ages between 3.8–4.2 Ga in lunar samples and meteorites, that appear to show an early heavy bombardment, consistent with formation of the Solar System, followed by a lull and then an uptick in the number of impact-affected ages. The common framing of two endmember models, a terminal cataclysm or a smooth, declining bombardment, is inadequate to explain all the data. The most parsimonious accounting may involve both an early phase of post-accretion bombardment and a later population of impactors generated by orbital instabilities of the outer planets.

Improved knowledge of the lunar cratering rate would yield better estimates for the ages of lunar terrains from which samples are not yet available. The goal is to obtain a much more complete knowledge of the impact history of the inner Solar System, including that of Earth; and reduce uncertainties in the ages of planetary surfaces throughout the Solar System. Key tests of the lunar bombardment scenarios include understanding whether the bombardment was a global phenomenon or an artifact of Imbrium basin ejecta contamination, the age distribution of the youngest and oldest basins, and whether the terrestrial planets and asteroid belt experienced a relative "lull" in impacts between early and late bombardment components. The relationship of the nearside lunar basins to one another is challenging for basin stratigraphy based on either cross-cutting relationships or visible crater statistics, because Imbrium basin's ejecta influenced the surrounding region so profoundly. Therefore, improvements to orbital remote sensing are unlikely to provide closure on this topic. Addressing these issues will require detailed geochronology of pre-Imbrian targets, accomplished by landing and in situ dating, and/or sample return to appropriate laboratories.

Having failed to definitively identify Nectaris or Crisium impact-melt materials in our current returned sample collection (see Section 2.1), these areas are prime candidates for sample-return or in situ dating missions to acquire absolute ages of these benchmark basins. Although the Nectaris and Crisium basins have experienced both basaltic infill and erosion, their original multiring morphologies are still recognizable. Updated geologic maps of the Nectaris basin and its surrounding terrain identify small plains near inner-basin ring massifs and inter-massif "draped" deposits as possible remnants of the Nectaris basin impact melt sheet (Smith and Spudis 2013; Spudis and Smith 2013). Similar efforts also identified small kipukas of the Crisium basin impact melt sheet, based on their morphology and composition (Spudis and Sliz 2017). In both Nectaris and Crisium, these small areas occur between the inner and outer basin rings. Some of the exposures exhibit cracked and fissured morphologies consistent with those at fresh craters (such as Tycho and King craters; Howard and Wilshire 1975) and older impact melts (e.g., Orientale; Wilhelms 1987; Spudis et al. 2014), and show embayment by subsequent mare basalt flows. The compositions of these areas, determined from Clementine data, indicate that they have less FeO than the surrounding basalts, attesting to their affinity to lunar highlands that were the pre-existing target materials. If these are indeed areas of preserved Nectaris or Crisium impact melt, such sites would be unique among basins as in situ impact melt exposures. In contrast to attempts to identify impact melt rocks thrown from the basin to distant sites like Apollo 17 or Luna 20, regolith formed atop an impact melt substrate would contain a majority of impact-melt rocks—more similar to finding basaltic materials in the regolith developed over Mare Tranquilitatis at Apollo 11.

As the oldest stratigraphically recognizable basin on the Moon, the SPA age anchors the early impact flux curve. The crater density on SPA ejecta is a factor of two higher than Nectaris, implying that the SPA basin did not form during the period of the lunar cataclysm, but instead formed during an earlier phase of lunar history (Marchi et al. 2012). The composition of the SPA interior is well-preserved in orbital remote sensing (Jolliff et al. 2000), providing a means to establish provenance for such samples. Impact-affected rocks derived from younger basins such as Apollo, Poincaré, Planck, Ingenii, Orientale and Schrödinger, as well as other large impact craters, would also contribute to establishing an impact chronology far from Imbrium that is bounded by the earliest and the latest of the recognized lunar impact basins. Sample return from major lunar basins continues to be a high priority goal in global lunar strategy documents (National Research Council 2003, 2007, 2011; Lunar Exploration Analysis Group 2017; International Space Exploration Coordination Group 2018).

Expanding the absolute chronological framework for the post-basin era will require additional radiometric dating of samples with well-established provenance, including young mare basalts and key stratigraphic craters such as Copernicus and Kepler (Ryder et al. 1989; Hiesinger et al. 2000; Morota et al. 2011; Öhman and Kring 2012; Krüger et al. 2016). In addition, continued work is needed to determine the geologic provenance of Apollo and Luna sampled units to understand sample ages, for example, understanding the Crisium lava flows and relating them to the Luna 24 samples (Nielsen and Drake 1978; Papike and Vaniman 1978).

Understanding the sources of projectiles bombarding the Moon projectile sources will also have important implications for understanding the dynamics of populations and temporal evolution of the Solar System. Such work may include returning samples from known basin impact melt deposits to help constrain both the nature of the projectile and when it struck the Moon, as well as searches for intact meteorite fragments. Promising targets for such searches include geochemical or physical anomalies related to impacts, for example, magnetic anomalies surrounding the South Pole-Aitken basin that may be concentrations of surviving impactor debris from nearside basins (Wieczorek et al. 2012), and impact crater central peaks with unusual mineralogical signatures that may be preferential sites for surviving projectiles (Yue et al. 2013). New laboratory methods to constrain the ages of regolith soils and breccias would be useful in understanding the temporal record of projectile delivery. The best temporally constrained records of regolith age are likely to be preserved in trapped ancient "paleoregolith" horizons found sandwiched between layers of radiometrically datable geological units such as lava flows, pyroclastic deposits, impact melt flows or ejecta blankets (Crawford et al. 2010; Fagents et al. 2010; Rumpf et al. 2013). However, such geological settings would require deep drilling (tens to hundreds of meters) capabilities to access the subsurface (Crawford et al. 2007; Crawford and Joy 2014).

Current lunar regolith gardening rates are derived from data taken near the Moon's equatorial plane. At high latitudes, where permanently shadowed regions exist, the meteoroid fluxes and subsequent impact gardening rates could be considerably different. A comprehensive model of lunar bombardment including all known sporadic sources such as the northern and southern toroidal sources would better address the impact gardening rates in these permanently shadowed regions. Continued operation of the LRO extended mission, as well as new missions with high-resolution imaging capabilities, increase the likelihood of finding more and larger impact events, helping better compare the recent flux with crater counting estimates. Lengthening the time difference between imaging sites under identical lighting conditions by LRO would improve the chances of imaging sites under different photometric geometries to help identify new craters.

REFERENCES

Abbott SS, Harrison TM, Schmitt AK, Mojzsis SJ (2012) A search for thermal excursions from ancient extraterrestrial impacts using Hadean zircon Ti–U–Th–Pb depth profiles. PNAS 109:13486–13492

Agnor CB, Lin D (2012) On the migration of Jupiter and Saturn: Constraints from linear models of secular resonant coupling with the terrestrial planets. Astrophys J 745:143

Andrews-Hanna JC, Besserer J, Head III JW, Howett CJ, Kiefer WS, Lucey PJ, McGovern PJ, Melosh HJ, Neumann GA, Phillips RJ, Schenk PM (2014) Structure and evolution of the lunar Procellarum region as revealed by GRAIL gravity data. Nature 514:68–71

Armstrong JC (2010) Distribution of impact locations and velocities of Earth meteorites on the Moon. Earth Moon Planets 107:43–54

Armstrong JC, Wells LE, Gonzalez G (2002) Rummaging through Earth's attic for remains of ancient life. Icarus 160:183–196

Arvidson R, Drozd R, Guinness E, Hohenberg C, Morgan C, Morrison R, Oberbeck V (1976) Cosmic ray exposure ages of Apollo 17 samples and the age of Tycho. Lunar Planet Sci Conf 7:2817–2832

Avdellidou C, Vaubaillon J (2019) Temperatures of lunar impact flashes: mass and size distribution of small impactors hitting the Moon. Mon Not R Astron Soc 484:5212–5222

Avdellidou C, Price MC, Delbo M, Cole MJ (2016) Survival of the impactor during hypervelocity collisions–II. An analogue for high-porosity targets. Mon Not R Astron Soc 464:734–738

Baker DM, Head JW, Collins GS, Potter RW (2016) The formation of peak-ring basins: Working hypotheses and path forward in using observations to constrain models of impact-basin formation. Icarus 273:146–163

Baldwin RB (2006) Was there ever a Terminal Lunar Cataclysm?: With lunar viscosity arguments. Icarus 184:308–318

Bandfield JL, Ghent RR, Vasavada AR, Paige DA, Lawrence SJ, Robinson MS (2011) Lunar surface rock abundance and regolith fines temperatures derived from LRO Diviner Radiometer data. J Geophys Res (Planets) 116

Barr AC, Canup RM (2010) Origin of the Ganymede-Callisto dichotomy by impacts during the late heavy bombardment. Nat Geosci 3:164–167

Barra F, Swindle TD, Korotev RL, Jolliff BL, Zeigler RA, Olson E (2006) ^{40}Ar/^{39}Ar dating of Apollo 12 regolith: Implications for the age of Copernicus and the source of nonmare materials. Geochim Cosmochim Acta 70:6016–6031

Basilevsky AT, Head JW (2012) Age of Giordano Bruno crater as deduced from the morphology of its secondaries at the Luna 24 landing site. Planet Space Sci 73:302–309

Bell EA, Harrison TM (2013) Post-Hadean transitions in Jack Hills zircon provenance: A signal of the Late Heavy Bombardment? Earth Planet Sci Lett 364:1–11

Bellucci JJ, Whitehouse MJ, Nemchin AA, Snape JF, Pidgeon RT, Grange M, Reddy SM, Timms N (2016) A scanning ion imaging investigation into the micron-scale U–Pb systematics in a complex lunar zircon. Chem Geol 438:112–122

Bernatowicz TJ, Hohenberg CM, Hudson B, Kennedy BM, Podosek FA (1978) Argon ages for lunar breccias 14064 and 15405. Proc Lunar Planet Sci Conf 9:905–919

Blichert-Toft J, Albarède F (2008) Hafnium isotopes in Jack Hills zircons and the formation of the Hadean crust. Earth Planet Sci Lett 265:686–702

Boehnke P, Harrison TM (2016) Illusory Late Heavy Bombardments. PNAS 113:10802

Bogard DD (2011) K–Ar ages of meteorites: Clues to parent-body thermal histories. Chemie der Erde 71:207–226

Bogard DD, Garrison DH, Shih CY, Nyquist LE (1994) ^{39}Ar–^{40}Ar dating of two lunar granites: the age of Copernicus. Geochim Cosmochim Acta 58:3093–3100

Bottke WF, Norman MD (2017) The Late Heavy Bombardment. Annu Rev Earth Planet Sci 45:619–647

Bottke WF, Levison HF, Nesvorny D, Dones L (2007) Can planetesimals left over from terrestrial planet formation produce the lunar Late Heavy Bombardment? Icarus 190:203–223

Bottke WF, Vokrouhlicky D, Minton D, Nesvorny D, Morbidelli A, Brasser R, Simonson B, Levison HF (2012) An Archaean heavy bombardment from a destabilized extension of the asteroid belt. Nature 485:78–81

Bouvier A, Wadhwa M, Korotev RL, Hartmann WK (2015) Pb–Pb chronometry of lunar impact melt breccias and comparison with other radiochronometric records. *In:* The First 1 Ga of Impact Records: Evidence from Lunar Samples and Meteorites:#6016

Brandon AD, Humayun M, Puchtel IS, Zolensky ME (2005) Re–Os isotopic systematics and platinum group element composition of the Tagish Lake carbonaceous chondrite. Geochim Cosmochim Acta 69:1619–1631

Cadogan PH, Turner G (1976) The chronology of the Apollo 17 Station 6 boulder. Proc Lunar Planet Sci Conf 7:2267–2285

Cadogan PH, Turner G (1977) ^{40}Ar–^{39}Ar dating of Luna 16 and Luna 20 samples. Philos Trans R Soc A 284:167–177

Cassata WS, Borg LE, Crow CA (2017) Thermochronometric constraints on basin-forming impact events from ^{40}Ar–^{39}Ar analysis of excavated crustal rocks. Lunar Planet Sci Conf 49:#1773

Cavosie AJ, Erickson TM, Timms NE, Reddy SM, Talavera C, Montalvo SD, Pincus MR, Gibbon RJ, Moser D (2015) A terrestrial perspective on using ex situ shocked zircons to date lunar impacts. Geology 43:999–1002

Chambers JE, Lissauer JJ (2002) A new dynamical model for the lunar late heavy bombardment. Lunar Planet Sci Conf 33:#1093

Chapman CR (2002) Planetary science: Earth's lunar attic. Nature 419:791–794

Chapman CR, Cohen BA, Grinspoon DH (2007) What are the real constraints on the existence and magnitude of the late heavy bombardment? Icarus 189:233–245

Cohen BA (2013) The Vestan cataclysm: Impact-melt clasts in howardites and the bombardment history of 4 Vesta. Meteorit Planet Sci 48:771–785

Cohen BA, Swindle TD, Kring DA (2000) Support for the lunar cataclysm hypothesis from lunar meteorite impact melt ages. Science 290:1754–1756

Cohen BA, Snyder GA, Hall CM, Taylor LA, Nazarov MA (2001) Argon-40-argon-39 chronology and petrogenesis along the eastern limb of the Moon from Luna 16, 20, and 24 samples. Meteorit Planet Sci 36:1345–1366

Cohen BA, Swindle TD, Kring DA (2005) Geochemistry and ^{40}Ar–^{39}Ar geochronology of impact-melt clasts in feldspathic lunar meteorites: Implications for lunar bombardment history. Meteorit Planet Sci 40:755–777

Conrad JW, Nimmo F, Neumann GA, Kamata S, Fassett CI (2016) Characterizing hidden impact basins discovered by GRAIL gravity data. Lunar Planet Sci Conf 47:#2208

Crawford IA, Baldwin EC, Taylor EA, Bailey JA, Tsembelis K (2008) On the survivability and detectability of terrestrial meteorites on the Moon. Astrobiology 8:242–252

Crawford IA, Fagents SA, Joy KH, Rumpf ME (2010) Lunar palaeoregolith deposits as recorders of the galactic environment of the solar system and implications for astrobiology. Earth Moon Planets 107:75–85

Crow CA, McKeegan KD, Moser DE (2017) Coordinated U–Pb geochronology, trace element, Ti-in-zircon thermometry and microstructural analysis of Apollo zircons. Geochim Cosmochim Acta 202:264–284

Ćuk M (2012) Chronology and sources of lunar impact bombardment. Icarus 218:69–79

Ćuk M, Gladman BJ, Stewart ST (2010) Constraints on the source of lunar cataclysm impactors. Icarus 207:590–594

Culler TS, Becker TA, Muller RA, Renne PR (2000) Lunar impact history from ^{40}Ar/^{39}Ar dating of glass spherules. Science 287:1785–1788

Curran NM, Nottingham M, Alexander L, Crawford IA, Füri E, Joy KH (2020) A database of noble gases in lunar samples in preparation for mass spectrometry on the Moon. Planet Space Sci 182:104823

Dalrymple GB, Ryder G (1993) ^{40}Ar/^{39}Ar age spectra of Apollo 15 impact melt rocks by laser step-heating and their bearing on the history of lunar basin formation. J Geophys Res 98:13,085–13,095

Dalrymple GB, Ryder G (1996) Argon-40/argon-39 age spectra of Apollo 17 highlands breccia samples by laser step heating and the age of the Serenitatis basin. J Geophys Res 101:26,069–26,084

Daly RT, Schultz PH (2016) Delivering a projectile component to the vestan regolith. Icarus 264:9–19

Day JM, Brandon AD, Walker RJ (2016) Highly siderophile elements in Earth, Mars, the Moon, and asteroids. Rev Mineral Geochem 81:161–238

Delano JW (1986) Pristine lunar glasses: criteria, data, and implications. J Geophys Res 91:201-D213

Delano JW (1991) Geochemical comparison of impact glasses from lunar meteorites ALHA81005 and MAC88105 and Apollo 16 regolith 64001. Geochim Cosmochim Acta 55:3019–3029

Delano JW, Zellner NEB, Barra F, Olson E, Swindle TD, Tibbetts NJ, Whittet DCB (2007) An integrated approach to understanding Apollo 16 impact glasses: Chemistry, isotopes, and shape. Meteorit Planet Sci 42:993–1004

Drozd RJ, Hohenberg CM, Morgan CJ, Podosek FA, Wroge ML (1977) Cosmic-ray exposure history at Taurus-Littrow. Proc Lunar Planet Sci Conf 8:3027–3043

Eberhardt P, Eugster O, Geiss J, Groegler N, Guggisberg S, Moergeli M (1976) Noble gases in the Apollo 16 special soils from the East-West split and the permanently shadowed area. Proc Lunar Planet Sci Conf 7:563–585

Eugster O, Groegler N, Mendia MD, Eberhardt P, Geiss J (1973) Trapped solar wind noble gases and exposure age of Luna 16 lunar fines. Geochim Cosmochim Acta 37:1991–2003

Eugster O, Geiss J, Grogler N (1983) Dating of early regolith exposure and the evolution of trapped ^{40}Ar/^{36}Ar with time. Lunar Planet Sci Conf 14:#177–178

Eugster O, Terribilini D, Polnau E, Kramers J (2001) The antiquity indicator argon-40/argon-36 for lunar surface samples calibrated by uranium-235-xenon-136 dating. Meteorit Planet Sci 36:1097–1115

Evans AJ, Soderblom JM, Andrews-Hanna JC, Solomon SC, Zuber MT (2016) Identification of buried lunar impact craters from GRAIL data and implications for the nearside maria. Geophys Res Lett 43:2445–2455

Fagan AL, Joy KH, Bogard DD, Kring DA (2014) Ages of globally distributed lunar paleoregoliths and soils from 3.9 Ga to the present. Earth Moon Planets 112:59–71

Fagents SA, Elise Rumpf M, Crawford IA, Joy KH (2010) Preservation potential of implanted solar wind volatiles in lunar paleoregolith deposits buried by lava flows. Icarus 207:595–604

Fassett CI (2016) Analysis of impact crater populations and the geochronology of planetary surfaces in the inner solar system. J Geophys Res (Planets) 121:1900–1926

Fassett CI, Minton DA (2013) Impact bombardment of the terrestrial planets and the early history of the Solar System. Nat Geosci 6:520–524

Fassett CI, Thomson BJ (2014) Crater degradation on the lunar maria: Topographic diffusion and the rate of erosion on the Moon. J Geophys Res (Planets) 119:2255–2271

Fassett CI, Head JW, Kadish SJ, Mazarico E, Neumann GA, Smith DE, Zuber MT (2012) Lunar impact basins: Stratigraphy, sequence and ages from superposed impact crater populations measured from Lunar Orbiter Laser Altimeter (LOLA) data. J Geophys Res 117

Featherstone WE, Hirt C, Kuhn M (2013) Band-limited Bouguer gravity identifies new basins on the Moon. J Geophys Res (Planets) 118:1397–1413

Fernandes VA, Fritz J, Weiss BP, Garrick-Bethell I, Shuster DL (2013) The bombardment history of the Moon as recorded by ^{40}Ar–^{39}Ar chronology. Meteorit Planet Sci 48:241–269

Fernandez J, Ip W-H (1984) Some dynamical aspects of the accretion of Uranus and Neptune: The exchange of orbital angular momentum with planetesimals. Icarus 58:109–120

Fischer-Gödde M, Becker H (2012) Osmium isotope and highly siderophile element constraints on ages and nature of meteoritic components in ancient lunar impact rocks. Geochim Cosmochim Acta 77:135–156

Frey H (2011) Previously unknown large impact basins on the Moon: Implications for lunar stratigraphy. *In*: Recent Advances and Current Research Issues in Lunar Stratigraphy. Ambrose WA, Williams DA (eds) Geological Society of America Special Paper. Vol 477, p 53–75

Garrick-Bethell I, Weiss BP, Shuster DL, Buz J (2009) Early lunar magnetism. Science 323:356

Garrick-Bethell I, Miljković K, Hiesinger H, van der Bogert CH, Laneuville M, Shuster DL, Korycansky DG (2020) Troctolite 76535: A sample of the Moon's South Pole-Aitken basin? Icarus 338:113430

Ghent RR, Hayne PO, Bandfield JL, Campbell BA, Allen CC, Carter LM, Paige DA (2014) Constraints on the recent rate of lunar ejecta breakdown and implications for crater ages. Geology 42:1059–1062

Gleißner P, Becker H (2017) Formation of Apollo 16 impactites and the composition of late accreted material: Constraints from Os isotopes, highly siderophile elements and sulfur abundances. Geochim Cosmochim Acta 200:1–24

Gleißner P, Becker H (2019) Origin of lunar fragmental matrix breccias—Highly siderophile element constraints. Meteorit Planet Sci 54:2006–2026

Gombosi DJ, Baldwin SL, Watson EB, Swindle TD, Delano JW, Roberge WG (2015) Argon diffusion in Apollo 16 impact glass spherules: Implications for ^{40}Ar/^{39}Ar dating of lunar impact events. Geochim Cosmochim Acta 148:251–268

Gomes R, Levison HF, Tsiganis K, Morbidelli A (2005) Origin of the cataclysmic Late Heavy Bombardment period of the terrestrial planets. Nature 435:466–469

Grange ML, Nemchin AA, Pidgeon RT, Timms N, Muhling JR, Kennedy AK (2009) Thermal history recorded by the Apollo 17 impact melt breccia 73217. Geochim Cosmochim Acta 73:3093–3107

Grange ML, Nemchin AA, Jourdan F (2010) Review of ages of lunar impact rocks: implication to the timing of Serenitatis and Imbrium Impacts and the LHB Model. Lunar Planet Sci Conf 41:#1533

Grange ML, Nemchin AA, Pidgeon RT (2013) The effect of 1.9 and 1.4 Ga impact events on 4.3 Ga zircon and phosphate from an Apollo 15 melt breccia. J Geophys Res (Planets) 118:2180–2197

Haack H, Farinella P, Scott ERD, Keil K (1996) Meteoritic, asteroidal, and theoretical constraints on the 500 Ma disruption of the L Chondrite parent body. Icarus 119:182–191

Harrison TM (2009) The Hadean Crust: Evidence from >4 Ga Zircons. Annu Rev Earth Planet Sci 37:479–505

Hartmann KW (2019) History of the Terminal Cataclysm Paradigm: Epistemology of a planetary bombardment that never (?) happened. Geosciences 9:285

Hartmann WK (1975) Lunar "cataclysm": A misconception? Icarus 24:181–187

Hartmann WK, Wood CA (1971) Moon: Origin and evolution of multi-ring basins. Moon 3:3–78

Hartmann WK, Ryder G, Dones L, Grinspoon D (2000) The time-dependent intense bombardment of the primordial Earth–Moon system. *In*: Origin of the Earth and Moon. Canup RM, Righter K (eds). University of Arizona Press, Tucson, p 493–512

Haruyama J, Ohtake M, Matsunaga T, Morota T, Honda C, Yokota Y, Abe M, Ogawa Y, Miyamoto H, Iwasaki A, Pieters CM (2009) Long-lived volcanism on the lunar farside revealed by SELENE Terrain Camera Science 323:905–908

Haskin LA, Korotev RL, Rockow KM, Jolliff BL (1998) The case for an Imbrium origin of the Apollo Th-rich impact-melt breccias. Meteorit Planet Sci 33:959–975

Head JW (1974) Stratigraphy of the Descartes region (Apollo 16): Implications for the origin of samples. Moon 11:77–99

Head JW, Adams JB, McCord TB, Pieters C, Zisk S (1978) Regional stratigraphy and geologic history of Mare Crisium. *In*: Mare Crisium: The View from Luna 24. Merrill RB, Papike JJ (eds). Pergamon Press, New York, p 43–74

Head JW, 3rd, Fassett CI, Kadish SJ, Smith DE, Zuber MT, Neumann GA, Mazarico E (2010) Global distribution of large lunar craters: implications for resurfacing and impactor populations. Science 329:1504–1507

Heck PR, Schmitz B, Baur H, Wieler R (2008) Noble gases in fossil micrometeorites and meteorites from 470 Myr old sediments from southern Sweden, and new evidence for the L-chondrite parent body breakup event. Meteorit Planet Sci 43:517–528

Heck PR, Ushikubo T, Schmitz B, Kita NT, Spicuzza MJ, Valley JW (2010) A single asteroidal source for extraterrestrial Ordovician chromite grains from Sweden and China: High-precision oxygen three-isotope SIMS analysis. Geochim Cosmochim Acta 74:497–509

Hiesinger H, Jaumann R, Neukam G, Head JW (2000) Ages of mare basalts on the lunar nearside. J Geophys Res 105:29239–29276

Hiesinger H, Head JW, Wolf U, Jaumann R, Neukum G (2003) Ages and stratigraphy of mare basalts in Oceanus Procellarum, Mare Nubium, Mare Cognitum, and Mare Insularum. J Geophys Res 108(E7):5065

Hiesinger H, van der Bogert CH, Pasckert JH, Funcke L, Giacomini L, Ostrach LR, Robinson MS (2012) How old are young lunar craters? J Geophys Res (Planets) 117:E00H10

Hiesinger H, Pasckert JH, van der Bogert CH, Robinson MS, Weinauer J, Lawrence SJ, Stopar JD, Robinson MS (2016) New crater size–frequency distribution measurements for Autolycus Crater, Moon. Lunar Planet Sci Conf 47:#1879

Hiesinger H, van der Bogert CH, Michael G, Schmedemann N, Iqbal W, Robbins SJ, Ivanov B, Williams J-P, Zanetti M, Plescia J, Ostrach LR, Head III JW (2023) The lunar cratering chronology. Rev Mineral Geochem 89:401–451

Holden P, Lanc P, Ireland TR, Harrison TM, Foster JJ, Bruce Z (2009) Mass-spectrometric mining of Hadean zircons by automated SHRIMP multi-collector and single-collector U/Pb zircon age dating: The first 100,000 grains. Inter J Mass Spectrom 286:53–63

Hörz F, Cintala M (1997) Impact experiments related to the evolution of planetary regoliths. Meteorit Planet Sci 32:179–209
Hörz F, Grieve R, Heiken G, Spudis P, Binder A (1991) Lunar surface processes. *In*: Lunar Sourcebook: A User's Guide to the Moon. Heiken GH, Vaniman DT, French BM (eds). Cambridge University Press, Cambridge, p 61–120
Howard KA, Wilshire HG (1975) Flows of impact melt at lunar craters. U S Geol Survey J Res 3:237–251
Hurwitz D, Kring DA (2016) Identifying the geologic context of Apollo 17 impact melt breccias. Earth Planet Sci Lett 436:64–70
International Space Exploration Coordination Group (2018) ISECG Global Exploration Roadmap (3rd edition). https://wwwglobalspaceexplorationorg/wordpress/wp-content/isecg/GER_2018_small_mobilepdf
Ishihara Y, Morota T, Nakamura R, Goossens S, Sasaki S (2011) Anomalous Moscoviense basin: Single oblique impact or double impact origin? Geophys Res Lett 38:L03021
James OB (1981) Petrologic and age relations of the Apollo 16 rocks: Implications for subsurface geology and the age of the Nectaris basin. Proc Lunar Planet Sci Conf 12:209–233
James OB (1996) Siderophile elements in lunar impact melts define nature of the impactors. Lunar Planet Sci Conf 27:#603–604
Jessberger EK, Kirsten T, Staudacher T (1976) Argon–argon ages of consortium breccia 73215. Proc Lunar Planet Sci Conf 7:2201–2215
Johnson BC, Melosh HJ (2012) Impact spherules as a record of an ancient heavy bombardment of Earth. Nature 485:75–77
Jolliff BL, Gillis JJ, Haskin LA, Korotev RL, Wieczorek MA (2000) Major lunar crustal terranes: Surface expressions and crust-mantle origins. J Geophys Res 105:4197–4216
Jourdan F (2012) The $^{40}Ar/^{39}Ar$ dating technique applied to planetary sciences and terrestrial impacts. Aust J Earth Sci 59:199–224
Joy KH, Arai T (2013) Lunar meteorites: New insights into the geological history of the Moon. Astron Geophys 54:4.28–24.32
Joy KH, Kring DA, Bogard DD, McKay DS, Zolensky ME (2011) Re-examination of the formation ages of the Apollo 16 regolith breccias. Geochim Cosmochim Acta 75:7208–7225
Joy KH, Zolensky ME, Nagashima K, Huss GR, Ross DK, McKay DS, Kring DA (2012) Direct detection of projectile relics from the end of the lunar basin-forming epoch. Science 336:1426-1429
Joy KH, Crawford IA, Curran NM, Zolensky M, Fagan AF, Kring DA (2016) The Moon: An archive of small body migration in the solar system. Earth Moon Planets 118:133–158
Joy KH, Tartèse R, Messenger S, Zolensky ME, Marrocchi Y, Frank DR, Kring DA (2020a) The isotopic composition of volatiles in the unique Bench Crater carbonaceous chondrite impactor found in the Apollo 12 regolith. Earth Planet Sci Lett 540:116265
Joy KH, Snape JF, Nemchin AA, Tartèse R, Martin DM, Whitehouse MJ, Vishnyakov V, Pernet-Fisher JF, Kring DA (2020b) Timing of geological events in the lunar highlands recorded in shocked zircon-bearing clasts from Apollo 16. R Soc Open Sci 7:200236200236
Joy KH, Gross J, Korotev RL, Zeigler RA, McCubbin FM, Snape JF, Curran NM, Pernet-Fisher JF, Arai T (2023) Lunar meteorites. Rev Mineral Geochem 89:509–562
Kaib NA, Chambers JE (2016) The fragility of the terrestrial planets during a giant-planet instability. Mon Not R Astron Soc 455:3561–3569
Kamata S, Sugita S, Abe Y, Ishihara Y, Harada Y, Morota T, Namiki N, Iwata T, Hanada H, Araki H, Matsumoto K (2015) The relative timing of Lunar Magma Ocean solidification and the Late Heavy Bombardment inferred from highly degraded impact basin structures. Icarus 250:492–503
Kennedy T, Jourdan F, Bevan AWR, Mary Gee MA, Frew A (2013) Impact history of the HED parent body(ies) clarified by new $^{40}Ar/^{39}Ar$ analyses of four HED meteorites and one anomalous basaltic achondrite. Geochim Cosmochim Acta 115:162–182
Kenny GG, Morales LF, Whitehouse MJ, Petrus JA, Kamber BS (2017) The formation of large neoblasts in shocked zircon and their utility in dating impacts. Geology 45:1003–1006
Koeberl C (2006) The record of impact processes on the early Earth: A review of the first 2.5 billion years. GSA Special Paper 405:1–22
Korochantseva EV, Buikin AI, Hopp J, Lorenz CA, Korochantsev AV, Ott U, Trieloff M (2016) Thermal and irradiation history of lunar meteorite Dhofar 280. Meteorit Planet Sci 51:2334–2346
Korotev RL (1987) The meteorite component of Apollo 16 noritic impact melt breccias. J Geophys Res 92:491–512
Korotev RL (1994) Compositional variation in Apollo 16 impact-melt breccias and inferences for the geology and bombardment history of the Central Highlands of the Moon. Geochim Cosmochim Acta 58:3931–3969
Korotev RL, Zeigler RA, Floss C (2010) On the origin of impact glass in the Apollo 16 regolith. Geochim Cosmochim Acta 74:7362–7388
Kring DA, Cohen BA (2002) Cataclysmic bombardment throughout the inner solar system 3.9–4.0 Ga. J Geophys Res 107(E2):5009
Krüger T, van der Bogert CH, Hiesinger H (2016) Geomorphologic mapping of the lunar crater Tycho and its impact melt deposits. Icarus 273:164–181
Lega E, Morbidelli A, Nesvorný D (2013) Early dynamical instabilities in the giant planet systems. Mon Not R Astron Soc 431:3494–3500
Levine J, Becker TA, Muller RA, Renne PR (2005) $^{40}Ar/^{39}Ar$ dating of Apollo 12 impact spherules. Geophys Res Lett 32:L15201

Levison HF, Dones L, Chapman CR, Stern SA, Duncan MJ, Zahnle K (2001) Could the lunar "Late Heavy Bombardment" have been triggered by the formation of Uranus and Neptune? Icarus 151:286–306

Liu D, Jolliff BL, Zeigler RA, Korotev RL, Wan Y, Xie H, Zhang Y, Dong C, Wang W (2012) Comparative zircon U–Pb geochronology of impact melt breccias from Apollo 12 and lunar meteorite SaU 169, and implications for the age of the Imbrium impact. Earth Planet Sci Lett 319–320:277–286

Liu J, Sharp M, Ash RD, Kring DA, Walker RJ (2015) Diverse impactors in Apollo 15 and 16 impact melt rocks: Evidence from osmium isotopes and highly siderophile elements. Geochim Cosmochim Acta 155:122–153

Lorenzetti S, Busemann H, Eugster O (2005) Regolith history of lunar meteorites. Meteorit Planet Sci 40:315

Lowe DR, Byerly GR, Kyte FT, Shukolyukov A, Asaro F, Krull A (2003) Spherule beds 3.47–3.24 billion years old in the Barberton Greenstone Belt, South Africa: A record of large meteorite impacts and their influence on early crustal and biological evolution. Astrobiology 3:7–48

Lucey PG, Blewett DT, Taylor GJ, Hawke BR (2000) Imaging of lunar surface maturity. J Geophys Res: Planets 105:20377–20386

Lunar Exploration Analysis Group (2017) Advancing Science of the Moon: Report of the Specific Action Team. https://www.lpi.usra.edu/leag/reports/ASM-SAT-Report-final.pdf

Madiedo JM, Ortiz JL, Morales N, Cabrera-Caño J (2014) A large lunar impact blast on 2013 September 11. Mon Not R Astron Soc 439:2364–2369

Marchi S, Mottola S, Cremonese G, Massironi M, Martellato E (2009) A new chronology for the Moon and Mercury. Astron J 137:4936–4948

Marchi S, Bottke WF, Kring DA, Morbidelli A (2012) The onset of the lunar cataclysm as recorded in its ancient crater populations. Earth Planet Sci Lett 325–326:27–38

Marchi S, Bottke WF, Cohen BA, Wünnemann K, Kring DA, McSween HY, De Sanctis MC, O'Brien DP, Schenk P, Raymond CA, Russell CT (2013) High-velocity collisions from the lunar cataclysm recorded in asteroidal meteorites. Nat Geosci 6:303–307

Marchi S, Bottke WF, Elkins-Tanton LT, Bierhaus M, Wuennemann K, Morbidelli A, Kring DA (2014) Widespread mixing and burial of Earth's Hadean crust by asteroid impacts. Nature 511:578–582

Maurer P, Eberhardt P, Geiss J, Grogler N, Stettler A (1978) Pre-Imbrian craters and basins: ages, compositions, and excavation depths of Apollo 16 breccias. Geochim Cosmochim Acta 42:1687–1720

Mazrouei S, Ghent RR (2017) Towards an understanding of initial crater rock populations: Boulder distribution around Copernicus Crater. Lunar Planet Sci Conf 48:#1964

McEwen AS, Moore JM, Shoemaker EM (1997) The Phanerozoic impact cratering rate: Evidence from the farside of the Moon. J Geophys Res: Planets 102:9231–9242

McIntosh EC, Day JMD, Liu Y, Jiskoot C (2020) Examining the compositions of impactors striking the Moon using Apollo impact melt coats and anorthositic regolith breccia meteorites. Geochim Cosmochim Acta 274:192–210

McKay DS, Bogard DD, Morris RV, Korotev RL, Johnson P, Wentworth SJ (1986) Apollo 16 regolith breccias: characterization and evidence of early formation in the mega-regolith. J Geophys Res 91:D277-D304

Melosh HJ (1989) Impact Cratering: A Geologic Process. Oxford University Press, New York

Mercer CM, Young KE, Weirich JR, Hodges KV, Jolliff BL, Wartho J-A, van Soest MC (2015) Refining lunar impact chronology through high spatial resolution ^{40}Ar–^{39}Ar dating of impact melts. Sci Adv 1:e1400050

Merle RE, Nemchin AA, Grange ML, Whitehouse MJ, Pidgeon RT (2014) High resolution U–Pb ages of Ca-phosphates in Apollo 14 breccias: Implications for the age of the Imbrium impact. Meteorit Planet Sci 49:2241–2251

Merle RE, Nemchin AA, Whitehouse MJ, Pidgeon RT, Grange ML, Snape JF, Thiessen F (2017) Origin and transportation history of lunar breccia 14311. Meteorit Planet Sci 52:842–858

Michael G, Basilevsky A, Neukum G (2018) On the history of the early meteoritic bombardment of the Moon: Was there a terminal lunar cataclysm? Icarus 302:80–103

Miljković K, Wieczorek MA, Collins GS, Laneuville M, Neumann GA, Melosh HJ, Solomon SC, Phillips RJ, Smith DE, Zuber MT (2013) Asymmetric distribution of lunar impact basins caused by variations in target properties. Science 342:724–726

Minton DA, Richardson JE, Fassett CI (2015) Re-examining the main asteroid belt as the primary source of ancient lunar craters. Icarus 247:172–190

Morbidelli A, Petit J-M, Gladman B, Chambers J (2001) A plausible cause of the late heavy bombardment. Meteorit Planet Sci 36:371–380

Morbidelli A, Levison HF, Tsiganis K, Gomes R (2005) Chaotic capture of Jupiter's Trojan asteroids in the early Solar System. Nature 435:462–465

Morbidelli A, Marchi S, Bottke WF, Kring DA (2012a) A sawtooth-like timeline for the first billion years of lunar bombardment. Earth Planet Sci Lett 355–356:144–151

Morbidelli A, Lunine JI, O'Brien DP, Raymond SN, Walsh KJ (2012b) Building terrestrial planets. Annu Rev Earth Planet Sci 40:251–275

Morbidelli A, Walsh KJ, O'Brien DP, Minton DA, Bottke WF (2015) The dynamical evolution of the asteroid belt. *In*: Asteroids IV. Michel P (ed) University of Arizona Press, Tucson, p 493–507

Morbidelli A, Nesvorny D, Laurenz V, Marchi S, Rubie DC, Elkins-Tanton L, Wieczorek M, Jacobson S (2018) The timeline of the lunar bombardment: Revisited. Icarus 305:262–276

Morgan JW, Laul JC, Krähenbühl U, Ganapathy R, Anders E, Trombka JI, Peterson LE, Reedy RC, Arnold JR (1972) Major impacts on the moon: Characterization from trace elements in Apollo 12 and 14 samples. Lunar Planet Sci Conf Proceedings 3:#1377

Morgan JW, Ganapathy R, Higuchi H, Kraehenbuehl U, Anders E (1974) Lunar Basins: Tentative characterization of projectiles, from meteoritic elements in Apollo 17 boulders. Proc Lunar Sci Conf 5th:1703–1736

Morgan JW, Walker RJ, Brandon AD, Horan MF (2001) Siderophile elements in Earth's upper mantle and lunar breccias: Data synthesis suggests manifestations of the same late influx. Meteorit Planet Sci 36:1257–1276

Morota T, Haruyama Ji, Honda C, Yokota Y, Ohtake M, Furumoto M (2008) Lunar apex–antapex cratering asymmetry as an impactor recorder in the Earth–Moon system. Advances in Space Research 42:285–288

Morota T, Haruyama J, Miyamoto H, Honda C, Ohtake M, Yokota Y, Matsunaga T, Hirata N, Demura H, Takeda H, Ogawa Y (2009) Formation age of the lunar crater Giordano Bruno. Meteorit Planet Sci 44:1115–1120

Morota T, Haruyama J, Ohtake M, Matsunaga T, Honda C, Yokota Y, Kimura J, Ogawa Y, Hirata N, Demura H, Iwasaki A (2011) Timing and characteristics of the latest mare eruption on the Moon. Earth Planet Sci Lett 302:255–266

Morota T, Ishihara Y, Sasaki S, Goossens S, Matsumoto K, Noda H, Araki H, Hanada H, Tazawa S, Kikuchi F, Ishikawa T (2015) Lunar mare volcanism: lateral heterogeneities in volcanic activity and relationship with crustal structure. Geol Soc London, Spec Publ 401:127–138

Morris RV (1978) The surface exposure "maturity" of lunar soils—Some concepts and Is/FeO compilation. Proc Lunar Planet Sci Conf 9:2287–2297

Muehlberger WR, Horz F, Sevier JR, Ulrich GE, Papike JJ (1980) Mission objectives for geological exploration of the Apollo 16 landing site. Lunar Highlands Crust:#1–49

Muller RA, Becker TA, Culler TS, Renne PR (2001) Solar system impact rates measured from lunar spherule ages. *In*: Accretion of extraterrestrial matter throughout Earth's history. Peucker-Ehrenbrink B, Schmitz B (eds). Kluwer Academic/Plenum Publishers, New York, NY, p 447–452

Nagaoka H, Takasawa S, Nakamura AM, Sangen K (2014) Degree of impactor fragmentation under collision with a regolith surface—Laboratory impact experiments of rock projectiles. Meteorit Planet Sci 49:69–79

National Research Council (2003) New Frontiers in Solar System Exploration. The National Academies Press, Washington, DC

National Research Council (2007) The Scientific Context for the Exploration of the Moon. The National Academies Press, Washington, DC

National Research Council (2011) Vision and Voyages for Planetary Science in the Decade 2013–2022. The National Academies Press, Washington, DC

Nemchin A, Timms N, Pidgeon R, Geisler T, Reddy S, Meyer C (2009) Timing of crystallization of the lunar magma ocean constrained by the oldest zircon. Nat Geosci 2:133–136

Nesvorný D, Vokrouhlický D (2016) Neptune's orbital migration was grainy, not smooth. Astrophys J 825:94

Nesvorný D, Roig F, Bottke WF (2017) Modeling the historical flux of planetary impactors. Astron J 153:103

Neukum GP (1984) Meteorite bombardment and dating of planetary surfaces. National Aeronautics and Space Administration, Washington, D.C

Neukum G, Ivanov BA (1994) Crater size distributions and impact probabilities on Earth from lunar, terrestrial-planet, and asteroid cratering data. *In*: Hazards due to Comets and Asteroids. Gehrels T, Matthews MS, Schumann AM (eds). University of Arizona Press, Tucson, p 359–416

Neukum G, Ivanov BA, Hartmann WK (2001) Cratering records in the inner solar system in relation to the lunar reference system. Space Sci Rev 96:55–86

Neumann GA, Zuber MT, Smith DE, Lemoine FG (1996) The lunar crust: Global structure and signature of major basins. J Geophys Res 101:16,841–16,863

Neumann GA, Zuber MT, Wieczorek MA, Head JW, Baker DM, Solomon SC, Smith DE, Lemoine FG, Mazarico E, Sabaka TJ, Goossens SJ (2015) Lunar impact basins revealed by Gravity Recovery and Interior Laboratory measurements. Sci Adv 1:e1500852

Nielsen RL, Drake MJ (1978) The case for at least three mare basalt magmas at the Luna 24 site. *In*: Mare Crisium: The View from Luna 24. Merrill RB, Papike JJ (eds). Pergamon Press, New York, p 419–428

Niihara T, Beard SP, Swindle TD, Schaffer LA, Miyamoto H, Kring DA (2019) Evidence for multiple 4.0–3.7 Ga impact events within the Apollo 16 collection. Meteorit Planet Sci 54:675–698

Norman MD (2009) The Lunar Cataclysm: Reality or "Mythconception"? Elements 5:23–28

Norman MD, Nemchin AA (2014) A 4.2 billion year old impact basin on the Moon: U–Pb dating of zirconolite and apatite in lunar melt rock 67955. Earth Planet Sci Lett 388:387–398

Norman MD, Bennett VC, Ryder G (2002) Targeting the impactors: siderophile element signatures of lunar impact melts from Serenitatis. Earth Planet Sci Lett 202:217–228

Norman MD, Duncan RA, Huard JJ (2006) Identifying impact events within the lunar cataclysm from ^{40}Ar–^{39}Ar ages and compositions of Apollo 16 impact melt rocks. Geochim Cosmochim Acta 70:6032–6049

Norman MD, Duncan RA, Huard JJ (2010) Imbrium provenance for the Apollo 16 Descartes terrain: Argon ages and geochemistry of lunar breccias 67016 and 67455. Geochim Cosmochim Acta 74:763–783

Norman MD, Adena KJD, Christy AG (2012) Provenance and Pb isotopic ages of lunar volcanic and impact glasses from the Apollo 17 landing site. Aust J Earth Sci 59:291–306

Norman MD, Taylor LA, Shih C-Y, Nyquist LE (2016) Crystal accumulation in a 4.2 Ga lunar impact melt. Geochim Cosmochim Acta 172:410–429
Nunes PD, Tatsumoto M, Unruh DM (1974) U–Th–Pb systematics of some Apollo 17 lunar samples, and implications for a lunar basin excavation chronology. Proc Lunar Sci Conf 5:1487–1514
Oberst J, Christou A, Suggs R, Moser D, Daubar IJ, McEwen AS, Burchell M, Kawamura T, Hiesinger H, Wünnemann K, Wagner R (2012) The present-day flux of large meteoroids on the lunar surface—A synthesis of models and observational techniques. Planet Space Sci 74:179–193
Öhman T, Kring DA (2012) Photogeologic analysis of impact melt-rich lithologies in Kepler crater that could be sampled by future missions. J Geophys Res (Planets) 117:E00H08
Ong L, Asphaug EI, Korycansky D, Coker RF (2010) Volatile retention from cometary impacts on the Moon. Icarus 207:578–589
Ortiz J, Sada P, Rubio LB, Aceituno F, Aceituno J, Gutierrez P, Thiele U (2000) Optical detection of meteoroidal impacts on the Moon. Nature 405:921–923
Ortiz J, Aceituno F, Quesada J, Aceituno J, Fernández M, Santos-Sanz P, Trigo-Rodríguez J, Llorca J, Martín-Torres F, Montañés-Rodríguez P (2006) Detection of sporadic impact flashes on the Moon: Implications for the luminous efficiency of hypervelocity impacts and derived terrestrial impact rates. Icarus 184:319–326
Ozima M, Miura YN, Podosek FA (2004) Orphan radiogenic noble gases in lunar breccias: evidence for planet pollution of the Sun? Icarus 170:17–23
Papike JJ, Vaniman DT (1978) Luna 24 ferrobasalts and the mare basalt suite: Comparative chemistry, mineralogy, and petrology. *In*: Mare Crisium: The View from Luna 24. Merrill RB, Papike JJ (eds). Pergamon Press, New York, p 371–401
Pidgeon RT, Nemchin AA, van Bronswijk W, Geisler T, Meyer C, Compston W, Williams IS (2007) Complex history of a zircon aggregate from lunar breccia 73235. Geochim Cosmochim Acta 71:1370–1381
Pierazzo E, Melosh HJ (2000) Understanding oblique impacts from experiments, observations, and modeling. Annu Rev Earth Planet Sci 28:141–167
Puchtel IS, Walker RJ, James OB, Kring DA (2008) Osmium isotope and highly siderophile element systematics of lunar impact melt breccias: Implications for the late accretion history of the Moon and Earth. Geochim Cosmochim Acta 72:3022–3042
Raymond SN, Izidoro A (2017) Origin of water in the inner Solar System: Planetesimals scattered inward during Jupiter and Saturn's rapid gas accretion. Icarus 297:134–148
Robbins SJ (2014) New crater calibrations for the lunar crater-age chronology. Earth Planet Sci Lett 403:188–198
Robinson MS, Boyd AK, Denevi BW, Lawrence SJ, McEwen AS, Moser DE, Povilaitis RZ, Stelling RW, Suggs RM, Thompson SD, Wagner RV (2015) New crater on the Moon and a swarm of secondaries. Icarus 252:229–235
Roig F, Nesvorný D (2015) The evolution of asteroids in the Jumping-Jupiter migration model. Astron J 150:186
Rubin AE (2012) Fragments of the lunar cataclysm. Science 336:1390
Rumpf ME, Fagents SA, Crawford IA, Joy KH (2013) Numerical modeling of lava-regolith heat transfer on the Moon and implications for the preservation of implanted volatiles. J Geophys Res (Planets) 118:382–397
Ryder G (1990) Lunar samples, lunar accretion, and the early bombardment of the Moon. Eos 71:313, 322–323
Ryder G (2002) Mass flux in the ancient Earth–Moon system and benign implications for the origin of life on Earth. J Geophys Res 107(E4):5022
Ryder G, Spudis PD, Taylor GJ (1989) The case for planetary sample return missions—Origin and evolution of the moon and its environment. EOS Trans 70:1495
Ryder G, Bogard D, Garrison D (1991) Probable age of Autolycus and calibration of lunar stratigraphy. Geology 19:143–146
Ryder G, Koeberl C, Mojzsis SJ (2000) Heavy bombardment on the Earth at ~3.85 Ga: The search for petrographic and geochemical evidence. *In*: Origin of the Earth and Moon. Canup RM, Righter K (eds) University of Arizona Press, Tucson, p 475–492
Schaeffer GA, Schaeffer OA (1977) Ar-39–Ar-40 ages of lunar rocks. Proc Lunar Planet Sci Conf 8:2253–2300
Schmitt HH, Petro NE, Wells RA, Robinson MS, Weiss BP, Mercer CM (2017) Revisiting the field geology of Taurus-Littrow. Icarus 298:2–33
Schultz PH, Crawford DA (2016) Origin and implications of non-radial Imbrium Sculpture on the Moon. Nature 535:391–394
Sharp M, Gerasimenko I, Loudin LC, Liu J, James OB, Puchtel IS, Walker RJ (2014) Characterization of the dominant impactor signature for Apollo 17 impact melt rocks. Geochim Cosmochim Acta 131:62–80
Shoemaker EM, Hackman RJ, Mikhailov ZK (1962) Stratigraphic basis for a lunar time scale. The Moon 14:289–300
Shuster DL, Balco G, Cassata WS, Fernandes VA, Garrick-Bethell I, Weiss BP (2010) A record of impacts preserved in the lunar regolith. Earth Planet Sci Lett 290:155–165
Simonson BM, Glass BP (2004) Spherule layers—Records of ancient impacts. Annu Rev Earth Planet Sci 32:329–361
Smith MC, Spudis PD (2013) Geological map of the Nectaris Basin and its deposits. Lunar Planet Sci Conf 44:#1248
Smith JM, Meyer C, Compston W, Williams IS (1986) 73235,82 (pomegranate): An assemblage of lunar zircon with unique overgrowth. Lunar Planet Sci Conf 17:#805–806
Smith DE, Zuber MT, Neumann GA, Mazarico E, Lemoine FG, Head III JW, Lucey PG, Aharonson O, Robinson MS, Sun X (2017) Summary of the results from the Lunar Orbiter Laser Altimeter after seven years in lunar orbit. Icarus 283:70–91

Snape JF, Nemchin AA, Grange ML, Bellucci JJ, Thiessen F, Whitehouse MJ (2016) Phosphate ages in Apollo 14 breccias: Resolving multiple impact events with high precision U–Pb SIMS analyses. Geochim Cosmochim Acta 174:13–29
Soderblom LA (1970) A model for small-impact erosion applied to the lunar surface. J Geophys Res 75:2655–2661
Soderblom LA, Lebofsky LA (1972) Technique for rapid determination of relative ages of lunar areas from orbital photography. J Geophys Res (1896–1977) 77:279–296
Sood R, Chappaz L, Melosh HJ, Howell KC, Milbury C, Blair DM, Zuber MT (2017) Detection and characterization of buried lunar craters with GRAIL data. Icarus 289:157–172
Speyerer EJ, Povilaitis RZ, Robinson MS, Thomas PC, Wagner RV (2016) Quantifying crater production and regolith overturn on the Moon with temporal imaging. Nature 538:215–218
Spudis PD (1993) The Geology of Multi-Ring Impact Basins: The Moon and Other Planets. Cambridge University Press, Cambridge
Spudis PD, Sliz MU (2017) Impact melt of the lunar Crisium multiring basin. Geophys Res Lett 44:1260–1265
Spudis PD, Smith MC (2013) Stratigraphy and composition of Nectaris Basin deposits. Lunar Planet Sci Conf 44:#1483
Spudis PD, Wilhelms DE, Robinson MS (2011) The Sculptured Hills of the Taurus Highlands: Implications for the relative age of Serenitatis, basin chronologies and the cratering history of the Moon. J Geophys Res 116
Spudis PD, Martin DJP, Kramer G (2014) Geology and composition of the Orientale Basin impact melt sheet. J Geophys Res (Planets) 119:19–29
Stettler A, Albarede F (1978) ^{39}Ar–^{40}Ar systematics of two sub-millimetre rock fragments from Mare Crisium. Earth Planet Sci Lett 38:401–406
Stöffler D, Ryder G (2001) Stratigraphy and isotope ages of lunar geologic units: Chronology and standard for the inner solar system. Space Sci Rev 96:9–54
Stöffler D, Bischoff A, Borchardt R, Burghele A, Deutsch A, Jessberger EK, Ostertag R, Palme H, Spettel B, Reimold WU, Wacker K (1985) Composition and evolution of the lunar crust in the Descartes Highlands, Apollo 16. Proc Lunar Planet Sci Conf 15:449–506
Stöffler D, Ryder G, Ivanov BA, Artemieva NA, Cintala MJ, Grieve RAF (2006) Cratering history and lunar chronology. Rev Mineral Geochem 60:519–596
Strom RG, Malhotra R, Ito T, Yoshida F, Kring DA (2005) The origin of planetary impactors in the inner solar system. Science 309:1847–1850
Stuart-Alexander DE, Howard KA (1970) Lunar Maria and circular basins—a review. Icarus 12:440–456
Suggs RM, Moser DE, Cooke WJ, Suggs RJ (2014) The flux of kilogram-sized meteoroids from lunar impact monitoring. Icarus 238:23–36
Svetsov VV, Shuvalov VV (2015) Water delivery to the Moon by asteroidal and cometary impacts. Planet Space Sci 117:444–452
Swindle TD, Isachsen CE, Weirich JR, Kring DA (2009) ^{40}Ar–^{39}Ar ages of H-chondrite impact melt breccias. Meteorit Planet Sci 44:747–762
Swindle TD, Kring DA, Weirich JR (2014) ^{40}Ar/^{39}Ar ages of impacts involving ordinary chondrite meteorites. Geological Society, London, Special Publications 378:333–347
Swindle TD, Spudis PD, Taylor GJ, Korotev RL, R. H. Nichols J (1991) Searching for Crisium Basin ejecta—Chemistry and ages of Luna 20 impact melts. Proc Lunar Planet Sci Conf 21:167–181
Symes SJK, Sears DWG, Taunton A, Akridge DG, Huang S, Benoit PH (1998) The crystalline lunar spherules: Their formation and implications for the origin of meteoritic chondrules. Meteorit Planet Sci 33:13–29
Szalay JR, Horányi M (2016) Lunar meteoritic gardening rate derived from in situ LADEE/LDEX measurements. Geophys Res Lett 43:4893–4898
Tera F, Papanstassiou DA, Wasserburg GJ (1974) Isotopic evidence for a terminal lunar cataclysm. Earth Planet Sci Lett 22:1–21
Thiessen F, Nemchin AA, Snape JF, Whitehouse MJ, Bellucci JJ (2017) Impact history of the Apollo 17 landing site revealed by U–Pb SIMS ages. Meteorit Planet Sci 52:584–611
Thommes EW, Duncan MJ, Levison HF (1999) The formation of Uranus and Neptune in the Jupiter–Saturn region of the Solar System. Nature 402:635–638
Timms NE, Reddy SM, Healy D, Nemchin AA, Grange ML, Pidgeon RT, Hart R (2012) Resolution of impact-related microstructures in lunar zircon: A shock-deformation mechanism map. Meteorit Planet Sci 47:120–141
Trail D, Mojzsis SJ, Harrison TM, Schmitt AK, Watson EB, Young ED (2007) Constraints on Hadean zircon protoliths from oxygen isotopes, Ti-thermometry, and rare earth elements. Geochem Geophys Geosystems 8: Q06014
Tsiganis K, Gomes R, Morbidelli A, Levison HF (2005) Origin of the orbital architecture of the giant planets of the Solar System. Nature 435:459–461
Turner G (1979) A Monte Carlo fragmentation model for the production of meteorites: Implications for gas retention ages. Proc Lunar Planet Sci Conf 10:1917–1941
Turner G, Cadogan PH, Yonge CJ (1973) Argon selenochronology. Proc Lunar Sci Conf 4th:1889–1914
van der Bogert CH, Hiesinger H, Spudis P (2017) The Age of the Crisium Impact Basin. *In:* New Views of the Moon 2 - Europe:##1988
Vaniman DT, Papike JJ (1980) Lunar highland melt rocks—Chemistry, petrology and silicate mineralogy. Lunar Highlands Crust:#271–337

Walker RJ, Bermingham K, Liu J, Puchtel IS, Touboul M, Worsham EA (2015) In search of late-stage planetary building blocks. Chem Geol 411:125–142
Walsh KJ, Morbidelli A, Raymond SN, O'brien DP, Mandell AM (2011) A low mass for Mars from Jupiter/'s early gas-driven migration. Nature 475:206–209
Wang J, Cheng W, Zhou C (2015) A Chang'E-1 global catalog of lunar impact craters. Planet Space Sci 112:42–45
Werner SC, Harris AW, Neukum G, Ivanov BA (2002) The near-Earth asteroid size–frequency distribution: A snapshot of the lunar impactor size–frequency distribution. Icarus 156:287–290
Wetherill GW (1975) Late heavy bombardment of the moon and terrestrial planets. Proc Lunar Planet Sci Conf 6:1539–1561
White LF, Černok A, Darling JR, Whitehouse MJ, Joy KH, Cayron C, Dunlop J, Tait KT, Anand M (2020) Evidence of extensive lunar crust formation in impact melt sheets 4,330 Myr ago. Nature Astronomy 10.1038/s41550-020-1092-5
Wichman R, Schultz P (1992) The Crisium basin: Implications of an oblique impact for basin ring formation and cavity collapse. Geological Society of America Special Papers 293:61–72
Wieczorek MA, Neumann GA, Nimmo F, Kiefer WS, Taylor GJ, Melosh HJ, Phillips RJ, Solomon SC, Andrews-Hanna JC, Asmar SW, Konopliv AS (2013) The crust of the Moon as seen by GRAIL. Science 339:671–675
Wieler R (2016) Do lunar and meteoritic archives record temporal variations in the composition of solar wind noble gases and nitrogen? A reassessment in the light of Genesis data. Chemie der Erde 76:463–480
Wilhelms DE (1987) The geologic history of the Moon. US Geological Survey Professional Paper 1348
Williams J-P, Pathare AV, Aharonson O (2014) The production of small primary craters on Mars and the Moon. Icarus 235:23–36
Xilouris EM, Bonanos AZ, Bellas-Velidis I, Boumis P, Dapergolas A, Maroussis A, Liakos A, Alikakos I, Charmandaris V, Dimou G, Fytsilis A (2018) NELIOTA: The wide-field, high-cadence, lunar monitoring system at the prime focus of the Kryoneri Telescope. Astron Astrophys 619
Yanagisawa M, Kisaichi N (2002) Lightcurves of 1999 Leonid impact flashes on the Moon. Icarus 159:31–38
Yue Z, Johnson BC, Minton DA, Melosh HJ, Di K, Hu W, Liu Y (2013) Projectile remnants in central peaks of lunar impact craters. Nat Geosci. 6:435–437
Zeigler RA, Korotev RL, Jolliff BL, Haskin LA, Floss C (2006) The geochemistry and provenance of Apollo 16 mafic glasses. Geochim Cosmochim Acta 70:6050–6067
Zellner NEB (2017) Cataclysm no more: New views on the timing and delivery of lunar impactors. Origins Life Evol Biosphere 47:261–280
Zellner NEB, Delano JW (2015) $^{40}Ar/^{39}Ar$ ages of lunar impact glasses: Relationships among Ar diffusivity, chemical composition, shape, and size. Geochim Cosmochim Acta 161:203–218
Zellner NEB, Spudis PD, Delano JW, Whittet DCB (2002) Impact glasses from the Apollo 14 landing site and implications for regional geology. J Geophys Res E107:5102
Zellner NEB, Delano JW, Swindle TD, Barra F, Olsen E, Whittet DCB (2009a) Apollo 17 regolith, 71501,262: A record of impact events and mare volcanism in lunar glasses. Meteorit Planet Sci 44:839–851
Zellner NEB, Delano JW, Swindle TD, Barra F, Olsen E, Whittet DCB (2009b) Evidence from $^{40}Ar/^{39}Ar$ ages of lunar impact glasses for an increase in the impact rate ~800 Ma ago. Geochim Cosmochim Acta 73:4590–4597
Zhang B, Lin Y, Moser DE, Hao J, Shieh SR, Bouvier A (2019) Imbrium age for zircons in Apollo 17 South Massif impact melt breccia 73155. J Geophys Res: Planets 124:3205–3218
Zuber MT, Smith DE, Watkins MM, Asmar SW, Konopliv AS, Lemoine FG, Melosh HJ, Neumann GA, Phillips RJ, Solomon SC (2013) Gravity field of the Moon from the Gravity Recovery and Interior Laboratory (GRAIL) mission. Science 339:668–671
Zuber MT, Smith DE, Neumann GA, Goossens S, Andrews-Hanna JC, Head JW, Kiefer WS, Asmar SW, Konopliv AS, Lemoine FG (2016) Gravity field of the Orientale basin from the Gravity Recovery and Interior Laboratory Mission. Science 354:438–441

APPENDIX—RECENT DEVELOPMENTS

Since the discovery of the Moon's asymmetric ejecta cloud, the origin of its sunward-canted density enhancement has not been well understood. Szalay et al. (2020) have proposed that Beta-meteoroids that hit the Moon's sunward side could explain this unresolved asymmetry. Beta-meteoroids are submicron in size, comparable to or smaller than the regolith particles they hit and can impact the Moon at very high speeds ~100 km s^{-1}. This finding suggests that Beta-meteoroids may also contribute to the evolution of other airless surfaces in the inner solar system, and by extension, at exozodiacal systems.

REFERENCE

Szalay JR, Pokorný P, Horányi M (2020) Hyperbolic meteoroids impacting the Moon. Astrophys J Lett 890:L11